

Dynamical spin structure factors of quantum spin nematic states

Ryuichi Shindou,^{1,2} Seiji Yunoki,³ and Tsutomu Momoi²

¹*Physics Department, Tokyo Institute of Technology, Ookayama, 2-12-1, Meguro-ku, Tokyo Japan*

²*Condensed Matter Theory Laboratory, RIKEN, 2-1 Hirosawa, Wako, Saitama 351-0198, Japan*

³*Computational Condensed Matter Laboratory, RIKEN, 2-1 Hirosawa, Wako, Saitama 351-0198, Japan*

(Dated: February 18, 2022)

Dynamical spin structure factors of quantum spin nematic states are calculated in a spin- $\frac{1}{2}$ square-lattice J_1 - J_2 model with ferromagnetic J_1 and competing antiferromagnetic J_2 interactions. To this end, we use a fermion representation, generalizing it to N flavors. We begin with a spin-triplet pairing state of fermion fields, called Z_2 planar state, which is a stable saddle-point solution in the large- N limit in a finite parameter range where the couplings J_1 and J_2 compete strongly [R. Shindou and T. Momoi, Phys. Rev. B **80**, 064410 (2009)]. Using a large- N expansion, we take into account fluctuations around this saddle point up to corrections of order $1/N$. The dynamical spin structure factors thus obtained signify the existence of gapless q -linear director-wave (spin-wave) modes at $\mathbf{q} = (0, 0)$ and gapped ‘gauge-field’ like collective modes at $\mathbf{q} = (\pi, \pi)$, whose spectral weight vanishes as a linear and quadratic function of the momentum respectively. The low-energy collective modes contain fluctuations of nematic-director, spin, and gauge degrees of freedom. Associated with the gapless q -linear modes, we evaluate the temperature dependence of the nuclear spin relaxation rate $1/T_1$ in the low-temperature regime as $1/T_1 \propto T^{2d-1}$, where d is the effective spatial dimension.

PACS numbers:

I. INTRODUCTION

Frustrated magnets are Mott insulators in which competing exchange interactions between localized spins bring about an extensively large degeneracy in the ground state energetics. In a certain circumstance, such a frustrated spin system lifts this degeneracy quantum-mechanically, only to choose as its ground state a liquid-like state of matter, dubbed a quantum spin liquid.¹⁻⁴ Typically, a ground-state wavefunction of quantum spin liquids consists of what we call spin-singlet valence bonds. A spin-singlet valence bond—a spin-singlet pair of two $S = 1/2$ spins—is energetically favored by an antiferromagnetic exchange interaction between the two spins. A ground-state wavefunction of quantum spin liquids is given by a quantum-mechanical superposition of different spatial partitionings of the spin-singlet valence bonds over the entire lattice, so that the state preserves not only the spin-rotational symmetry but also the lattice translational symmetry.²

Having no symmetry-breaking order parameter, quantum spin liquids have been regarded as a new quantum state of matter, which should be sharply contrasted from conventional magnetic phases such as a Néel ordered phase and a valence bond solid phase.¹ In fact, owing to its fluid-like feature, the spin liquid phase has various unconventional low-energy excitations, such as a ‘gauge-field’ like collective excitation and a fractionalized (or ‘individual’) magnetic excitation called spinon.^{3,4} Experimental and theoretical searches for this new non-magnetic phase have been intensively carried out in the past couple of decades in the field of quantum magnetism.

Another new quantum state of matter recently explored in localized spin systems is a quantum spin nematic phase,⁵⁻²² which is a quantum-spin analogue of

nematic liquid-crystal phases. Spin nematic states neither possess any spin order, i.e. sublattice magnetization, nor any crystalline solid-like structure in spin degrees of freedom, but, unlike spin-rotational symmetric quantum spin liquids, they exhibit various types of spin anisotropy, whose order parameters are given by symmetric rank-2 traceless spin tensor operators⁵

$$Q_{j\mathbf{m},\mu\nu} = \frac{1}{2}(S_{j,\mu}S_{\mathbf{m},\nu} + S_{j,\nu}S_{\mathbf{m},\mu}) - \frac{\delta_{\mu\nu}}{3}\mathbf{S}_j \cdot \mathbf{S}_{\mathbf{m}} \quad (1)$$

for $\mu, \nu = x, y, z$. Here $\mathbf{S}_j = (S_{j,x}, S_{j,y}, S_{j,z})$ denotes the spin-1/2 vector operator on site j . The tensor operator (1) consists of two spin operators defined on different sites j and \mathbf{m} , usually neighboring two sites, so that the order parameter is defined on bond (j, \mathbf{m}) . This order is hence called a ‘bond-type’ spin nematic order. Ground-state wavefunctions of this phase can be essentially described as quantum-mechanical superpositions of different spatial partitionings of both spin-singlet valence bonds and a part of spin-triplet valence bonds,⁹ so that quantum spin nematics can be regarded as ‘cousins’ of symmetric quantum spin liquids, possibly sharing many of their exotic characters. At the same time, they should have gapless collective modes—Nambu-Goldstone modes—due to the broken spin-rotational symmetries, which is distinct from the quantum spin liquids.

Recently, various theoretical investigations have revealed the appearance of spin nematic phases in several frustrated spin-1/2 magnets that have both ferromagnetic couplings and competing antiferromagnetic couplings.⁶⁻¹⁹ Among two-dimensional systems, ground-state properties of the spin-1/2 J_1 - J_2 model on the square lattice have been reasonably most studied. The Hamil-

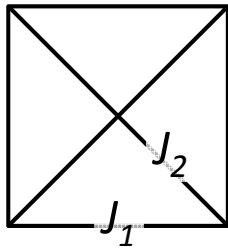


FIG. 1: Square-lattice J_1 - J_2 frustrated ferromagnetic model, in which the nearest-neighbor exchange J_1 is ferromagnetic and the next-nearest-neighbor exchange J_2 is antiferromagnetic.

tonian is given by

$$H = -J_1 \sum_{\langle i,j \rangle} \mathbf{S}_i \cdot \mathbf{S}_j + J_2 \sum_{\langle\langle i,j \rangle\rangle} \mathbf{S}_i \cdot \mathbf{S}_j \quad (2)$$

with ferromagnetic J_1 and antiferromagnetic J_2 ($J_1, J_2 > 0$), where the first (second) summation runs over all pairs of nearest-neighbor (next-nearest-neighbor) sites (see Fig. 1). It has been proposed^{8,26} that a spin nematic phase appears in a finite parameter range around $J_2/J_1 = 0.5$. In contrast to theoretical developments, experimental verifications of spin nematic phases have just started, especially in quasi-one-dimensional systems, but they are still very limited.^{20–22} One of the difficulties for experimentally detecting this new phase is the absence of any direct probe for the spin quadratic order parameter Eq. (1) and the lack of theoretical understanding²³ of characteristic properties in this phase.

The purpose of this paper is to clarify dynamical properties of a quantum spin nematic phase and to give a relevant physical characterization to this new class of quantum spin states. To this end, we generalize the J_1 - J_2 model to an N -flavor J_1 - J_2 spin model, using a fermion representation.⁹ In this approach, wavefunctions of spin-nematic ground states are described with spin-triplet pairings of fermion fields, whose d -vectors specify the spin-nematic director vectors associated with the quadrupolar moments.

The classical ($S \rightarrow \infty$) phase diagram of the square-lattice J_1 - J_2 model with ferromagnetic J_1 consists of only two phases; a collinear antiferromagnetic phase in the strong antiferromagnetic J_2 regime and a ferromagnetic phase in the strong ferromagnetic J_1 regime. In the quantum ($S = 1/2$) system, it has been argued that the quantum spin nematic phase emerges in between these two magnetic ordered phases.⁸ The previous saddle point analysis⁹ of the spin-1/2 J_1 - J_2 model concluded that, for large N , a certain spin nematic phase dubbed Z_2 planar phase²⁴ stably appears in ground states in a finite parameter range where ferromagnetic J_1 couplings strongly compete with antiferromagnetic J_2 couplings (see Fig. 2). In this pairing state, the spin-triplet d -vectors introduced on ferromagnetic bonds take a coplanar spatial configuration, which by itself mimics the pairing symmetry of

a two-dimensional analogue of Balian-Werthamer state²⁵ in Helium-3 superfluid B phase. It was demonstrated that the wavefunction of this Z_2 planar state reasonably reproduces the d -wave spin nematic state proposed by the previous exact diagonalization study.⁸ The Z_2 planar state possesses the same spatial configuration of quadrupolar orders on bonds as the d -wave spin nematic state and also both of the states have the same spatial symmetries.²⁶ A variational Monte Carlo study²⁶ based on mean-field solutions further indicated that, when projected onto the physical $S = 1/2$ spin Hilbert space, the optimized Z_2 planar state achieves the best optimal energy in the original ($N = 1$) spin-1/2 J_1 - J_2 model in a finite parameter range, compared with other competing states. Among various mean-field ansatzes, only the Z_2 planar phase (spin nematic phase) survives, except for the ferromagnetic and collinear antiferromagnetic phases, after the projection. The d -wave bond spin nematic phase is hence expected to appear in the spin-1/2 J_1 - J_2 model for any number N .

In this paper, we calculate dynamical magnetic properties of the quantum spin nematic phase in a generalized N -flavor spin-1/2 J_1 - J_2 model on the square lattice. Employing a $1/N$ expansion for large N , we take into account fluctuations around the mean-field (saddle-point) solutions. The treatment up to order of $1/N$ essentially corresponds to the so-called random phase approximation (RPA). The dynamical spin structure factors $\text{Im}\chi_{\mu\mu}(\mathbf{q}, \epsilon)$ ($\mu = x, y, z$) thus calculated have two characters; a spin-liquid-like character and a symmetry-broken-phase character. The former feature manifests itself as the Stoner continuum of the individual excitations of free spinons. The latter character is represented by gapless collective modes, which have q -linear energy dispersions. The gapless collective modes are given by long-wavelength fluctuations of nematic directors. For finite momenta, these director excitations are accompanied with weak spin excitations, which are measurable through small but finite spectral weight in the dynamical spin structure factor. The spectral weight of $\text{Im}\chi_{\mu\mu}(\mathbf{q}, \epsilon)$ vanishes as a linear function of the momentum near the gapless point, e.g. $\text{Im}\chi_{zz}(\mathbf{q}, \epsilon) \simeq a_z v_z |\mathbf{q}| \delta(\epsilon - v_z |\mathbf{q}|) + \dots$, where v_z denotes the director-wave velocity and a_z is a finite constant. We further calculated NMR spin relaxation rate $1/T_1$ given by the gapless magnetic modes. Because the only physical magnetic low-energy modes are these gapless director-wave excitations around $\mathbf{q} = (0, 0)$, these excitations can induce a relatively slow spin relaxation, which has a temperature dependence $T_1^{-1} \propto T^{2d-1}$ in the low- T limit in d dimensions.

We further discuss how the Z_2 planar state changes to different states at the boundaries to the neighboring phases in the large N limit, analyzing the excitation modes. When the antiferromagnetic coupling J_2 decreases, the mean-field solution transforms from the Z_2 planar state to a $U(1)$ planar state at $J_2/J_1 = J_{c,2}$ (see Fig. 2). The calculation to first order in $1/N$ reveals that two gapped ‘gauge-field’ collective modes at

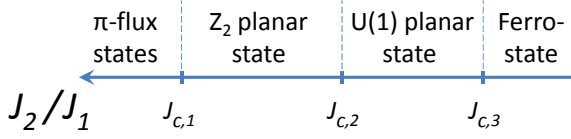


FIG. 2: Mean-field phase diagram of the $S = 1/2$ square-lattice J_1 - J_2 model in the large- N limit. In the strong J_2 regime, the mean-field ground state consists of only two decoupled spin-singlet pairing states defined on J_2 bonds, which are often called π -flux states.^{3,4,27} When ferromagnetic J_1 increases, the mean-field ground state acquires finite spin-triplet pairing amplitudes on the ferromagnetic bonds, which connect the decoupled π -flux states.⁹ These states are called Z_2 planar state and $U(1)$ planar state, depending on the amplitude of singlet pairings, and both of them are characterized as spin-nematic states. In the strong J_1 regime, the mean-field ground state contains only spin-triplet pairings, which corresponds to a fully-polarized ferromagnetic state (FM state).²⁶ Energetics of the mean-field solutions conclude that $J_{c,1} = 1.325$, $J_{c,2} = 1.0448$ and $J_{c,3} = 1.02$.

$\mathbf{q} = (\pi, \pi)$ become gapless at the transition point, only to constitute a compact QED (quantum electrodynamics) action in the $U(1)$ phase ($J_2/J_1 < J_{c,2}$), where the space-time instanton effect associated with this effective action introduces a strong confining potential between ‘free’ gapped spinons. This suggests that the finite mass at $\mathbf{q} = (\pi, \pi)$ in the Z_2 planar state quantifies the stability against the confinement effect. Inside the $U(1)$ planar phase, a couple of other bosonic modes simultaneously exhibit instabilities. Due to these instabilities, the $U(1)$ phase would break various symmetries such as the time-reversal symmetry, a spin- π -rotational symmetry and the translational symmetries.

The organization of this paper is as follows: In the next section, we first introduce a generalized N -flavor spin-1/2 quantum frustrated ferromagnetic model, whose large- N limit possesses our previous mean-field solutions as the exact ground states and whose $N = 1$ case safely reproduces the usual quantum spin- $\frac{1}{2}$ model. In Sec. III, we describe the $1/N$ -expansion calculation for the dynamical spin correlation functions. In Sec. IV, we show the calculated dynamical spin structure factors, both $\text{Im}\chi_{zz}(\mathbf{q}, \epsilon)$ and $\text{Im}\chi_{+-}(\mathbf{q}, \epsilon)$, and discuss their characteristic features and physical implications. We also discuss the nature of the $U(1)$ planar state here. Section V contains a calculation of NMR spin relaxation rate $1/T_1$. Section VI is devoted to the summary and discussion.

II. QUANTUM FRUSTRATED FERROMAGNETIC MODEL AND ITS LARGE- N LIMIT ON A SQUARE LATTICE

In this section, we describe our generalized $S = 1/2$ N -flavor J_1 - J_2 model. We also briefly review the Z_2 planar ground state, which is a stable saddle-point solution in the large- N limit of the present model in a finite parameter range of a strongly competing regime.

A. N -flavor spin-1/2 J_1 - J_2 model

The Hamiltonian for the generalized N -flavor spin-1/2 J_1 - J_2 model is given by⁹

$$\mathcal{H} = -\frac{J_1}{N} \sum_{\langle j, \mathbf{m} \rangle} \sum_{a, b=1}^N (\mathbf{S}_j^{ab} \cdot \mathbf{S}_{\mathbf{m}}^{ba} + \psi_j^{ab} \psi_{\mathbf{m}}^{ba}) + \frac{J_2}{N} \sum_{\langle\langle j, \mathbf{m} \rangle\rangle} \sum_{a, b} \mathbf{S}_j^{ab} \cdot \mathbf{S}_{\mathbf{m}}^{ba} + \sum_{j, a} \mathbf{h}_j^{aa} \cdot \mathbf{S}_j^{aa}, \quad (3)$$

where $\langle j, \mathbf{m} \rangle$ ($\langle\langle j, \mathbf{m} \rangle\rangle$) runs over all nearest-neighbor (2nd-neighbor) bonds on the square lattice, and the spin operators $\mathbf{S}_j^{ab} = (S_{j,1}^{ab}, S_{j,2}^{ab}, S_{j,3}^{ab})$ and the density operator ψ_j^{ab} are given by

$$\begin{aligned} S_{j,+}^{ab} &\equiv \frac{1}{2} (f_{j,\uparrow}^{a\dagger} f_{j,\downarrow}^b + f_{j,\uparrow}^{b\dagger} f_{j,\downarrow}^a), \\ S_{j,-}^{ab} &\equiv \frac{1}{2} (f_{j,\downarrow}^{a\dagger} f_{j,\uparrow}^b + f_{j,\downarrow}^{b\dagger} f_{j,\uparrow}^a), \\ S_{j,3}^{ab} &\equiv \frac{1}{2} (f_{j,\uparrow}^{a\dagger} f_{j,\uparrow}^b - f_{j,\downarrow}^{a\dagger} f_{j,\downarrow}^b), \\ \psi_j^{ab} &\equiv \frac{i}{2} (f_{j,\alpha}^{a\dagger} f_{j,\alpha}^b - f_{j,\alpha}^{b\dagger} f_{j,\alpha}^a). \end{aligned} \quad (4)$$

Here $f_{j,\alpha}^{a\dagger}$ is a fermion creation operator with spin $\alpha = \uparrow, \downarrow$ and flavor $a = 1, \dots, N$ on site $\mathbf{j} = (j_x, j_y)$. In this paper, we consider the case J_1 is ferromagnetic and J_2 is antiferromagnetic, i.e. $J_1 > 0$ and $J_2 > 0$. We have introduced external magnetic field $\mathbf{h}_j^{aa} = (h_{j,1}^{aa}, h_{j,2}^{aa}, h_{j,3}^{aa})$ to calculate the spin correlation function. The physical spin Hilbert space satisfies the local constraints

$$\sum_{a=1}^N f_{j,\alpha}^{a\dagger} f_{j,\alpha}^a = N, \quad \sum_{a=1}^N f_{j,\alpha}^a f_{j,\beta}^a \epsilon_{\alpha\beta} = 0 \quad (5)$$

on each site with $\epsilon_{\uparrow\downarrow} = -\epsilon_{\downarrow\uparrow} = 1$ and $\epsilon_{\uparrow\uparrow} = -\epsilon_{\downarrow\downarrow} = 0$, which endows the fermionic Hilbert space with the local $SU(2)$ gauge symmetry. The repeated spin indices imply their summations, whereas we write the summations for the flavor indices explicitly.

We note that, when $N = 1$, the Hamiltonian Eq. (3) in the physical Hilbert space reduces to the usual spin-1/2 J_1 - J_2 quantum Heisenberg model. We regard N to be large when we perform a $1/N$ expansion.

An equivalent statistical-mechanics problem at temperature β^{-1} can be formulated in terms of the path-integral representation. We decouple four-fermion interaction terms into a quadratic form, using Hubbard-Stratonovich-type transformation. Introducing scalar auxiliary fields ($\chi_{j\mathbf{m}}$ and $\eta_{j\mathbf{m}}$) for the antiferromagnetic interaction and vector auxiliary fields [$\mathbf{E}_{j\mathbf{m}} = (E_{j\mathbf{m},1}, E_{j\mathbf{m},2}, E_{j\mathbf{m},3})$ and $\mathbf{D}_{j\mathbf{m}} = (D_{j\mathbf{m},1}, D_{j\mathbf{m},2}, D_{j\mathbf{m},3})$] for the ferromagnetic interaction,⁹ we obtain the partition function in the form

$$Z[h] = \int \mathcal{D}\Psi^{a\dagger} \mathcal{D}\Psi^a \mathcal{D}\mathbf{a}_\tau \mathcal{D}U^{\sin} \mathcal{D}U^{\text{tri}} \exp \left(- \int_0^\beta d\tau \mathcal{L}[h, U^{\sin}, U^{\text{tri}}, \mathbf{a}_\tau] \right), \quad (6)$$

$$\begin{aligned} \mathcal{L} = \sum_{a=1}^N \left\{ \frac{1}{2} \sum_j \text{tr} \left[\Psi_j^{a\dagger} \left(\partial_\tau + \sum_{\mu=1}^3 i a_{j,\tau}^\mu \sigma_\mu \right) \Psi_j^a \right] - \frac{J_1}{4} \sum_{\langle j,m \rangle} \left(-|E_{jm}|^2 - |D_{jm}|^2 + \sum_{\mu=1}^3 \text{tr} [\Psi_j^{a\dagger} U_{jm,\mu}^{\text{tri}} \Psi_m^a \sigma_\mu^T] \right) \right. \\ \left. - \frac{J_2}{4} \sum_{\langle\langle j,m \rangle\rangle} \left(-|\chi_{jm}|^2 - |\eta_{jm}|^2 + \text{tr} [\Psi_j^{a\dagger} U_{jm}^{\sin} \Psi_m^a] \right) + \frac{1}{4} \sum_j \sum_{\mu=1}^3 h_{j,\mu}^{aa} \text{tr} [\Psi_j^{a\dagger} \Psi_j^a \sigma_\mu^T] \right\}, \quad (7) \end{aligned}$$

where the fermion fields are written in the 2×2 matrix form

$$\Psi_j^{a\dagger} \equiv \begin{bmatrix} f_{j,\uparrow}^{a\dagger} & f_{j,\downarrow}^a \\ f_{j,\downarrow}^{a\dagger} & -f_{j,\uparrow}^a \end{bmatrix} \quad (8)$$

and the auxiliary fields are included into the 2×2 matrices U_{jm}^{\sin} and $U_{jm}^{\text{tri}} = (U_{jm,1}^{\text{tri}}, U_{jm,2}^{\text{tri}}, U_{jm,3}^{\text{tri}})$ in the forms

$$U_{jm}^{\sin} \equiv \begin{bmatrix} \chi_{jm}^* & \eta_{jm}^* \\ \eta_{jm} & -\chi_{jm} \end{bmatrix}, \quad U_{jm,\mu}^{\text{tri}} \equiv \begin{bmatrix} E_{jm,\mu}^* & D_{jm,\mu}^* \\ -D_{jm,\mu} & E_{jm,\mu} \end{bmatrix} \quad (9)$$

($\mu = 1, 2, 3$). The trace denoted by the symbol “tr” is taken over 2×2 matrices such as Ψ_j^a and the Pauli matrices σ_μ . A Gaussian integral over the auxiliary fields exactly reproduces the original Hamiltonian given in Eq. (3). Integrating over the temporal gauge fields $\mathbf{a}_{j,\tau} = (a_{j,\tau}^1, a_{j,\tau}^2, a_{j,\tau}^3)$ also strictly imposes the local constraints given by Eq. (5) on every site and time.

As the Lagrangian is written in a quadratic form of fermion fields, we can formally rewrite the effective action as

$$\begin{aligned} \int_0^\beta d\tau \mathcal{L} = N \mathcal{S}_I \\ + \frac{1}{2} \sum_{\mathbf{k}, n, a} \mathbf{f}_{\mathbf{k}, n}^{a\dagger} \cdot \mathbf{G}_{(\mathbf{k}, n | \mathbf{k}', n')}^{-1} [h^{aa}, U^{\sin}, U^{\text{tri}}, \mathbf{a}_\tau] \cdot \mathbf{f}_{\mathbf{k}', n'}^a, \quad (10) \end{aligned}$$

where

$$\begin{aligned} \mathcal{S}_I \equiv \int_0^\beta d\tau \left[\frac{J_1}{4} \sum_{\langle j,m \rangle} (|E_{jm}|^2 + |D_{jm}|^2) \right. \\ \left. + \frac{J_2}{4} \sum_{\langle\langle j,m \rangle\rangle} (|\chi_{jm}|^2 + |\eta_{jm}|^2) \right] \quad (11) \end{aligned}$$

and \mathbf{G} denotes a 4×4 matrix single-particle Green function of the fermion field $\mathbf{f}_{\mathbf{k}, n}^{a\dagger}$ written in the Nambu representation

$$\mathbf{f}_{\mathbf{k}, n}^{a\dagger} \equiv \begin{pmatrix} f_{\mathbf{k}, n, \uparrow}^{a\dagger} & f_{\mathbf{k}, n, \downarrow}^{a\dagger} & f_{-\mathbf{k}, -n, \uparrow}^a & f_{-\mathbf{k}, -n, \downarrow}^a \end{pmatrix} \quad (12)$$

with

$$f_{\mathbf{k}, n, \sigma}^{a\dagger} \equiv \frac{1}{\sqrt{\beta N_\Lambda}} \sum_j \int_0^\beta d\tau e^{i\mathbf{k} \cdot \mathbf{j} + i\omega_n \tau} f_{j, \sigma}^{a\dagger}(\tau). \quad (13)$$

Here, N_Λ denotes the total number of lattice sites, $\mathbf{k} = (k_x, k_y)$, $\omega_n \equiv (2n+1)\pi\beta^{-1}$, and $\sigma = \uparrow, \downarrow$. Note that the functional $\mathbf{G}^{-1}[h^{aa}, U^{\sin}, U^{\text{tri}}, \mathbf{a}_\tau]$ is a linear function of the elements of h^{aa} , U^{\sin} , U^{tri} , and \mathbf{a}_τ .

The integral over the Ψ (\mathbf{f}) fields in Eq. (10) leads to the following partition function,

$$Z[h] = \int \mathcal{D}U^{\sin} \mathcal{D}U^{\text{tri}} \mathcal{D}\mathbf{a}_\tau \exp(-N\mathcal{S}[h, U^{\sin}, U^{\text{tri}}, \mathbf{a}_\tau]), \quad (14)$$

$$\mathcal{S} \equiv \mathcal{S}_I + \mathcal{S}_{\text{II}}, \quad (15)$$

$$\mathcal{S}_{\text{II}} \equiv -\frac{1}{2N} \sum_{a=1}^N \text{Tr}(\ln \mathbf{G}^{-1}[h^{aa}, U^{\sin}, U^{\text{tri}}, \mathbf{a}_\tau]), \quad (16)$$

where the Green function \mathbf{G} is diagonal in the flavor index and the trace of $\ln \mathbf{G}^{-1}$ is taken over the momentum (\mathbf{k}), the Matsubara frequency (ω_n), and the index of the 4×4 matrices, i.e., the spin and particle-hole indices.

B. Saddle point solution: Z_2 planar state

For large N , \mathcal{S}_{II} , as well as \mathcal{S}_I , is a functional of order unity, and the same is for \mathcal{S} . In the large N limit, since the prefactor of the action \mathcal{S} in Eq. (14) is proportional to the number N , the partition function (14) is governed by the saddle point solution of the fields U^{\sin} , U^{tri} , and \mathbf{a}_τ , which satisfies

$$\frac{\delta \mathcal{S}}{\delta U^{\sin}} = \frac{\delta \mathcal{S}}{\delta U^{\text{tri}}} = \frac{\delta \mathcal{S}}{\delta \mathbf{a}_\tau} = 0, \quad (17)$$

and the fluctuations of U^{\sin} , U^{tri} , and \mathbf{a}_τ are weak.

This saddle point solution indeed corresponds to the mean-field solution derived in Ref. 9. At the saddle point, the vector auxiliary fields $\mathbf{D}_{j\mathbf{l}}$ and $\mathbf{E}_{j\mathbf{l}}$, respectively, relate to the d -vectors of spin-triplet pairing and spin-triplet hopping, i.e.,

$$\bar{D}_{j\mathbf{l}, \mu} = i \langle f_{j, \alpha} [\sigma_2 \sigma_\mu]_{\alpha\beta} f_{\mathbf{l}, \beta} \rangle, \quad \bar{E}_{j\mathbf{l}, \mu} = \langle f_{j, \alpha}^\dagger [\sigma_\mu]_{\alpha\beta} f_{\mathbf{l}, \beta} \rangle \quad (18)$$

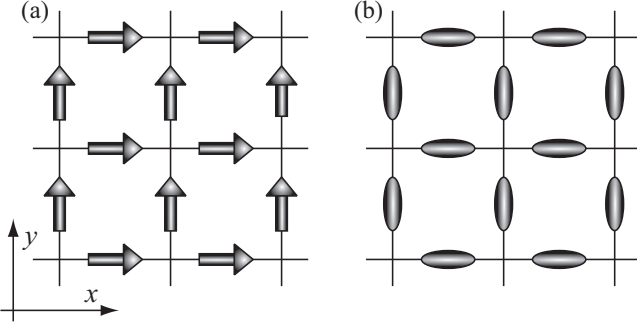


FIG. 3: Configurations of (a) d -vectors for spin triplet pairings and (b) directors corresponding to the quadrupolar moments in the Z_2 planar state on the square lattice.

($\mu = 1, 2, 3$), while the scalar auxiliary fields η_{jl} and χ_{jl} relate to the spin-singlet pairing and hopping, i.e.,

$$\bar{\eta}_{jl} = -i\langle f_{j,\alpha}[\sigma_2]_{\alpha\beta}f_{l,\beta} \rangle, \quad \bar{\chi}_{jl} = \langle f_{j,\alpha}^\dagger f_{l,\alpha} \rangle. \quad (19)$$

The present authors⁹ previously investigated various local minima of the action at zero magnetic field, $h = 0$, assuming that U^{sin} , U^{tri} , and \mathbf{a}_τ are temporally uniform and also preserve the translational symmetries of the square lattice. We found that, in an intermediate-coupling regime, the saddle point solution acquires finite spin-triplet pairings on the ferromagnetic bonds, while singlet pairings on the antiferromagnetic bonds. In particular, a coplanar configuration of orthogonal d -vectors in spin-triplet pairings on the ferromagnetic bonds [see Fig. 3(a)] on top of the ‘ π -flux’-type singlet pairings²⁷ on the antiferromagnetic bonds realizes the best mean-field energy among others.⁹ The solution is given by

$$\begin{aligned} \bar{U}_{\langle j,j+\mathbf{e}_x \rangle,\mu}^{\text{tri}} &\equiv i\delta_{\mu,1}D\sigma_2, & \bar{U}_{\langle j,j+\mathbf{e}_y \rangle,\mu}^{\text{tri}} &\equiv i\delta_{\mu,2}D\sigma_2, \\ \bar{U}_{\langle j,j+\mathbf{e}_x \pm \mathbf{e}_y \rangle}^{\text{sin}} &\equiv \chi\sigma_3 \pm \eta\sigma_1, & \bar{a}_{j,\tau}^\mu &= 0 \end{aligned} \quad (20)$$

with certain real values D , χ , and η , where $\mathbf{e}_x = (1, 0)$ and $\mathbf{e}_y = (0, 1)$. The presence of the d -vectors, $\bar{\mathbf{D}}_{\langle j,j+\mathbf{e}_x \rangle} = (D, 0, 0)$ and $\bar{\mathbf{D}}_{\langle j,j+\mathbf{e}_y \rangle} = (0, D, 0)$ [Fig. 3(a)], produces a quadrupolar order on bonds; in the mean-field approximation, we have the relation⁹

$$\begin{aligned} Q_{jl,\mu\nu} &= -\frac{1}{2} \left(E_{jl,\mu} E_{jl,\nu}^* - \frac{1}{3} \delta_{\mu\nu} |\mathbf{E}_{jl}|^2 \right) + \text{H.c.} \\ &\quad - \frac{1}{2} \left(D_{jl,\mu} D_{jl,\nu}^* - \frac{1}{3} \delta_{\mu\nu} |\mathbf{D}_{jl}|^2 \right) + \text{H.c.} \end{aligned} \quad (21)$$

($\mu, \nu = 1, 2, 3$). Hence the state has an antiferro-quadrupolar order, as shown in Fig. 3(b), where all nematic directors are lying in a single plane. The invariant gauge group³ dictates that all the gauge excitations around this mean-field solution have finite gap [are not required to be gapless by the local $SU(2)$ gauge symmetry]. The state has the same spin-triplet pairing function as a ‘planar’ type superfluid B-phase of ³He.³⁵ We hence dubbed this state the Z_2 planar state.

Here we summarize the symmetry of the Z_2 planar state. The wavefunction is invariant under the space translation and the space reflections with x - and y -axes. The state is also invariant under the time reversal \mathcal{T} ; under the operation of \mathcal{T} , the triplet pairings on the nearest neighbor links change their sign, but this change sets off by a staggered gauge transformation $\Psi_j^\dagger \rightarrow (-1)^{j_x+j_y} \Psi_j^\dagger$. This concludes that this state does not have any spin order i.e. $\langle \mathbf{S}_j \rangle = 0$.^{9,26} The coplanar ordering of the d -vectors breaks the $SU(2)$ spin-rotational symmetry, but the state preserves the spin π rotational symmetry around both 1-, 2-, and 3-axes. This corresponds to the fact that the ground-state manifold of the d -wave spin nematic state⁸ has $SU(2)/(Z_2 \times Z_2)$ symmetry. We also note that this pairing state has a non-trivial *staggered* $U(1)$ spin-rotational symmetry. That is, the state defined by Eq. (20) is invariant under the following staggered spin rotation about z axis

$$\begin{aligned} \Psi_j^\dagger &\rightarrow \exp[i(-1)^{j_x+j_y}\theta\sigma_3]\Psi_j^\dagger, \\ \Psi_j &\rightarrow \Psi_j \exp[-i(-1)^{j_x+j_y}\theta\sigma_3] \end{aligned} \quad (22)$$

for any θ .

This Z_2 planar state is shown to be a stable local minimum, even when projected onto the real spin space. A variational Monte Carlo study indicates that the projected BCS wavefunction constructed from this Z_2 planar state achieves the best optimal energy in the parameter range $0.42J_1 \leq J_2 \leq 0.57J_1$, which is encompassed by the competing ferromagnetic phase ($J_2 < 0.42J_1$) and collinear antiferromagnetic phase ($0.57J_1 < J_2$).²⁶ Moreover, the wavefunction of the projected Z_2 planar state belongs to the same space group (including its irreducible representation)²⁶ as that of the bond-type spin nematic phase suggested by the exact diagonalization analysis⁸ in the similar parameter regime. The spin correlation function calculated with this projected BCS wavefunction²⁶ exhibits a similar behavior as those obtained from the exact diagonalization studies up to 40 sites.²⁸ Observing the energetics and the consistencies with the previous exact diagonalization analyses, we regard that this projected Z_2 planar phase is indeed realized as a spin nematic phase in a certain parameter range around $J_2 \approx 0.5J_1$ of the present J_1 - J_2 model. We therefore start from the mean-field Z_2 planar state, to derive the dynamical magnetic properties of the bond-type spin nematic phase.

C. Partition function and Green function at the saddle point

We describe the partition function at the saddle point, omitting the fluctuations of U^{sin} , U^{tri} , and \mathbf{a}_τ in Eq. (6). The Bogoliubov–de Gennes Hamiltonian for the mean-field Z_2 planar state is given by

$$\mathbf{H}_\mathbf{k}^{(0)} \equiv \frac{J_1 D}{2} (s_x \gamma_3 - s_y \gamma_5) + J_2 (\chi c_x c_y \gamma_4 + \eta s_x s_y \gamma_2) \quad (23)$$

with $s_\mu \equiv \sin k_\mu$ and $c_\mu \equiv \cos k_\mu$ ($\mu = x, y$). The 4×4 γ -matrices are defined as

$$\gamma_1 = \sigma_2 \otimes \sigma_1 = \begin{pmatrix} 0 & -i\sigma_1 \\ i\sigma_1 & 0 \end{pmatrix}, \quad (24)$$

where the 2×2 Pauli matrices σ_μ ($\mu = 1, 2, 3$) in front of the \otimes -mark is for the particle-hole space, while the other is for the spin space. Using the same notation, we define the other 4 anti-commuting γ -matrices as $\gamma_2 = \sigma_2 \otimes \sigma_2$, $\gamma_3 = \sigma_2 \otimes \sigma_3$, $\gamma_4 = \sigma_3 \otimes \sigma_0$, and $\gamma_5 = \sigma_1 \otimes \sigma_0$.

The partition function at the saddle point takes the form

$$Z^{(0)}[h] = \exp \left(-N\mathcal{S}^{(0)}[h] \right), \quad (25)$$

$$\mathcal{S}^{(0)}[h] = \mathcal{S}_I^{(0)} + \mathcal{S}_{II}^{(0)}[h], \quad (26)$$

$$\mathcal{S}_I^{(0)} = \frac{\beta}{2} [J_1 N_\Lambda D^2 + J_2 N_\Lambda (\chi^2 + \eta^2)], \quad (27)$$

$$\mathcal{S}_{II}^{(0)}[h] = -\frac{1}{2N} \sum_{a=1}^N \text{Tr} \left(\ln \mathbf{G}_{0,(\mathbf{k},n,a|\mathbf{k}',n',a)}^{-1}[h] \right), \quad (28)$$

where the trace is over the momentum (\mathbf{k}), the Matsubara frequency (n), spin, and particle-hole indices. The single-particle Green function $\mathbf{G}_0[h]$ of the fermion fields $\mathbf{f}_{\mathbf{k},n}^a$ at the saddle point is given by

$$\begin{aligned} \mathbf{G}_{0,(\mathbf{k},n,a|\mathbf{k}',n',a)}^{-1}[h^{aa}] &\equiv \delta_{n,n'} \delta_{\mathbf{k},\mathbf{k}'} \mathbf{g}_0^{-1}(\mathbf{k}, i\omega_n) \\ &+ \frac{1}{2\sqrt{\beta N_\Lambda}} \sum_{\mu=1,2,3} \sum_{\mathbf{q},m} \delta_{\mathbf{k},\mathbf{k}'+\mathbf{q}} \delta_{n,n'+m} h_\mu^{aa}(\mathbf{q}, m) \mathbf{u}_\mu, \end{aligned} \quad (29)$$

where \mathbf{g}_0 denotes the 4×4 matrix single-particle Green function of $\mathbf{f}_{\mathbf{k},n}^a$ at zero field,

$$\mathbf{g}_0(\mathbf{k}, i\omega_n) \equiv \left(i\omega_n \gamma_0 - \mathbf{H}_\mathbf{k}^{(0)} \right)^{-1}, \quad (30)$$

\mathbf{u}_μ ($\mu = 1, 2, 3$) denote the 4×4 Hermite matrices defined by

$$\begin{aligned} \mathbf{u}_1 &\equiv \gamma_{15} = -i\gamma_1\gamma_5, & \mathbf{u}_2 &\equiv \gamma_{13} = -i\gamma_1\gamma_3, \\ \mathbf{u}_3 &\equiv \gamma_{35} = -i\gamma_3\gamma_5, \end{aligned} \quad (31)$$

and

$$h_\mu^{aa}(\mathbf{q}, m) \equiv \frac{1}{\sqrt{\beta N_\Lambda}} \sum_j \int_0^\beta d\tau e^{-i\mathbf{q} \cdot \mathbf{j} - i\epsilon_m \tau} h_{j,\mu}^{aa}(\tau) \quad (32)$$

with $\epsilon_m \equiv 2m\pi\beta^{-1}$. Diagonalizing the Hamiltonian matrix, we obtain the mean-field band dispersion relation of spinons,

$$\xi_\mathbf{k} = \left[\frac{J_1^2 D^2}{4} (s_x^2 + s_y^2) + J_2^2 (\chi^2 c_x^2 c_y^2 + \eta^2 s_x^2 s_y^2) \right]^{1/2}, \quad (33)$$

which has a full gap in the whole Brillouin zone, as shown in Fig. 4(a). When we expand the Green function \mathbf{G}_0 with small fields $\{h_\mu^{aa}\}$, the matrix \mathbf{u}_μ corresponds to the external vertex connecting the external field h_μ^{aa} with two single-particle Green functions \mathbf{g}_0 .

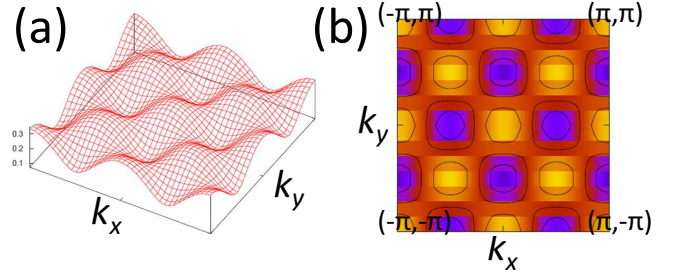


FIG. 4: (a) Dispersion relation of spinon band $\xi_\mathbf{k}$ in the Z_2 planar state at $J_2 = 1.1J_1$. (b) Contour plot of $\xi_\mathbf{k}$, showing 8 minima at $\mathbf{k} = (\pm\frac{\pi}{2}, 0), (0, \pm\frac{\pi}{2}), (\pm\frac{\pi}{2}, \pi), (\pi, \pm\frac{\pi}{2})$, and 8 maxima at $\mathbf{k} = (0, 0), (\pm\frac{\pi}{2}, \pm\frac{\pi}{2}), (0, \pi), (\pi, 0), (\pi, \pi)$.

III. $1/N$ EXPANSION FOR CORRELATION FUNCTIONS

In the previous section, we have described the saddle point solution of a generalized N -flavor spin-1/2 frustrated ferromagnetic model. For large N , the fluctuations of the auxiliary fields and the gauge fields around the saddle point are weak and hence they can be precisely included by performing a perturbational expansion of the effective action with the fluctuation fields. This expansion gives a $1/N$ expansion of physical quantities. In this section, performing this $1/N$ expansion, we calculate the dynamical spin correlation function²⁹

$$\begin{aligned} C_{\mu\nu}^{aa}(\mathbf{j}, \tau) &\equiv \langle T_\tau [S_{0,\mu}^{aa}(0) S_{\mathbf{j},\nu}^{aa}(\tau)] \rangle \Big|_{h=0} \\ &= \frac{\partial^2 Z[h]}{\partial h_{0,\mu}^{aa}(0) \partial h_{\mathbf{j},\nu}^{aa}(\tau)} \Big|_{h=0} \end{aligned} \quad (34)$$

and the dynamical susceptibility

$$\chi_{\mu\nu}^{aa}(\mathbf{q}, i\epsilon_m) = \sum_j \int_0^\beta d\tau e^{-i(\mathbf{q} \cdot \mathbf{j} + \epsilon_m \tau)} C_{\mu\nu}^{aa}(\mathbf{j}, \tau), \quad (35)$$

where T_τ denotes the imaginary-time ordering and the flavor index a is fixed to a certain number. Specifically, the correlation function of leading order, $O(1)$, corresponds to the Hartree-Fock contribution and the correction term of order $1/N$ corresponds to the random phase approximation (RPA) term. We present a formalism for this large N expansion here and discuss the dynamical spin structure factors thus obtained in the next section.

The spin correlation functions are composed by two parts

$$C_{\mu\nu}^{aa}(\mathbf{j}, \tau) = C_{\mu\nu,I}^{aa}(\mathbf{j}, \tau) + C_{\mu\nu,II}^{aa}(\mathbf{j}, \tau) \quad (36)$$

with

$$C_{\mu\nu,\text{I}}^{aa}(\mathbf{j}, \tau) \equiv -\frac{N}{Z} \int \mathcal{D}U^{\text{sin}} \mathcal{D}U^{\text{tri}} \mathcal{D}\mathbf{a}_\tau \times \frac{\partial^2 \mathcal{S}}{\partial h_{0,\mu}^{aa}(0) \partial h_{\mathbf{j},\nu}^{aa}(\tau)} \exp(-N\mathcal{S}) \Big|_{h=0}, \quad (37)$$

$$C_{\mu\nu,\text{II}}^{aa}(\mathbf{j}, \tau) \equiv \frac{N^2}{Z} \int \mathcal{D}U^{\text{sin}} \mathcal{D}U^{\text{tri}} \mathcal{D}\mathbf{a}_\tau \times \frac{\partial \mathcal{S}}{\partial h_{0,\mu}^{aa}(0)} \frac{\partial \mathcal{S}}{\partial h_{\mathbf{j},\nu}^{aa}(\tau)} \exp(-N\mathcal{S}) \Big|_{h=0}, \quad (38)$$

and they relate to corresponding dynamical susceptibilities

$$\chi_{\mu\nu,\text{I}}^{aa}(\mathbf{q}, i\epsilon_m) \equiv \sum_{\mathbf{j}} \int_0^\beta d\tau e^{-i(\mathbf{q} \cdot \mathbf{j} + \epsilon_m \tau)} C_{\mu\nu,\text{I}}^{aa}(\mathbf{j}, \tau),$$

$$\chi_{\mu\nu,\text{II}}^{aa}(\mathbf{q}, i\epsilon_m) \equiv \sum_{\mathbf{j}} \int_0^\beta d\tau e^{-i(\mathbf{q} \cdot \mathbf{j} + \epsilon_m \tau)} C_{\mu\nu,\text{II}}^{aa}(\mathbf{j}, \tau).$$

A. Correlation functions in the leading order

Replacing \mathcal{S} in Eqs. (37) and (38) by \mathcal{S}_0 given in Eqs. (26), (27), and (28), we obtain the Hartree-Fock contribution to the spin correlation function,

$$C_{\mu\nu}^{aa,(0)}(\mathbf{j}, \tau) = \left(-N \frac{\partial^2 \mathcal{S}^{(0)}}{\partial h_{0,\mu}^{aa}(0) \partial h_{\mathbf{j},\nu}^{aa}(\tau)} + N^2 \frac{\partial \mathcal{S}^{(0)}}{\partial h_{0,\mu}^{aa}(0)} \frac{\partial \mathcal{S}^{(0)}}{\partial h_{\mathbf{j},\nu}^{aa}(\tau)} \right) \Big|_{h=0}, \quad (39)$$

or equivalently,

$$\begin{aligned} \chi_{\mu\nu}^{aa,(0)}(\mathbf{q}, i\epsilon_m) &= -\frac{1}{8\beta N_\Lambda} \sum_{\mathbf{k}, n} \text{Tr}[\mathbf{g}_0(\mathbf{k} + \mathbf{q}, i\omega_n + i\epsilon_m) \mathbf{u}_\mu \mathbf{g}_0(\mathbf{k}, i\omega_n) \mathbf{u}_\nu] \\ &+ \frac{\delta_{\mathbf{q},0} \delta_{m,0}}{16\beta N_\Lambda} \left(\sum_{\mathbf{k}, n} \text{Tr}[\mathbf{g}_0(\mathbf{k}, i\omega_n) \mathbf{u}_\mu] \right) \\ &\times \left(\sum_{\mathbf{k}', n'} \text{Tr}[\mathbf{g}_0(\mathbf{k}', i\omega_{n'}) \mathbf{u}_\nu] \right), \end{aligned} \quad (40)$$

where the traces are taken over the spin and particle-hole indices, i.e., the indices of 4×4 matrices. From Eqs. (23), (30), and (31), it is clear that $\mathbf{g}_0(\mathbf{k}, i\omega_n) \mathbf{u}_\mu$ is traceless for each $\mu = 1, 2, 3$, and hence the second term vanishes. The first term corresponds to two spinons propagating with momenta $\mathbf{k} + \mathbf{q}$ and $-\mathbf{k}$ [see Fig. 5(d)].

After the analytic continuation, $i\epsilon_n \rightarrow \epsilon + i\delta$, we obtain the real-time dynamical susceptibilities. At zero temperature, the imaginary parts of dynamical susceptibilities

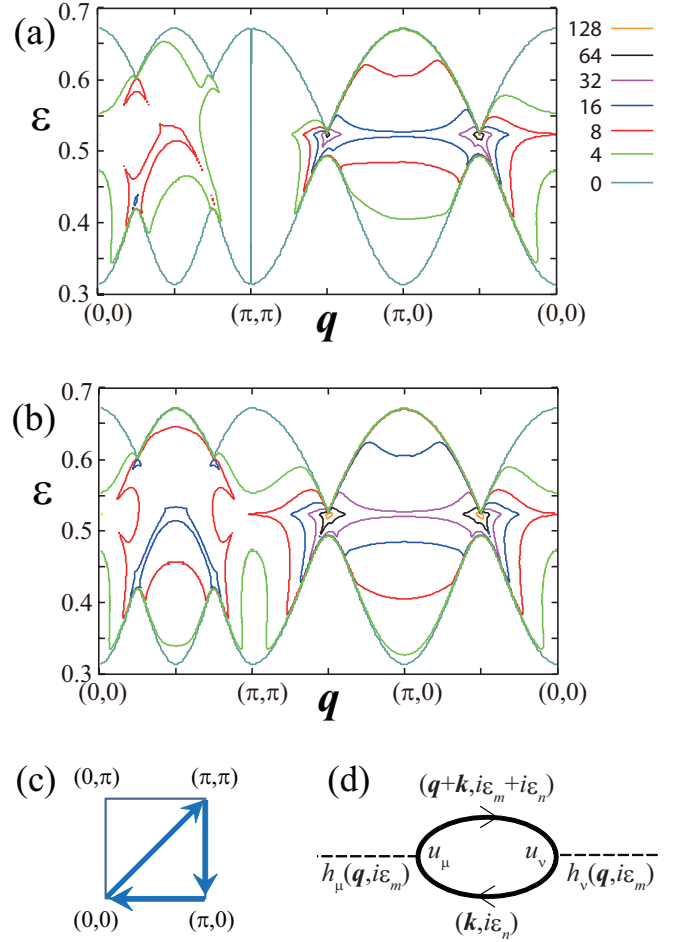


FIG. 5: Contour plots of (a) $\text{Im}\chi_{zz}^{(0)}(\mathbf{q}, \epsilon)$ and (b) $\text{Im}\chi_{+-}^{(0)}(\mathbf{q}, \epsilon)$ at $J_2 = 1.1J_1$. Both of them consist of broad continuum spectra, which have finite weight only for $\epsilon \geq \omega_c \simeq 0.3$. (c) Path of the momentum \mathbf{q} in (a) and (b), which runs from $(0,0)$ to (π,π) , to $(\pi,0)$ and back to $(0,0)$. (d) Feynman diagram for $\text{Im}\chi_{\mu\mu}^{(0)}(\mathbf{q}, i\epsilon_m)$. Solid lines denote the fermion single-particle Green functions and dashed lines denote the external magnetic fields.

at the saddle point are given by

$$\text{Im}\chi_{zz}^{(0)}(\mathbf{q}, \epsilon) = \frac{\pi}{8N_\Lambda} \sum_{\mathbf{k}} \delta(\epsilon - \xi_+ - \xi_-) \left[1 - \frac{1}{\xi_+ \xi_-} \times (a_{2,+} a_{2,-} - a_{3,+} a_{3,-} + a_{4,+} a_{4,-} - a_{5,+} a_{5,-}) \right], \quad (41)$$

$$\text{Im}\chi_{+-}^{(0)}(\mathbf{q}, \epsilon) = \frac{\pi}{4N_\Lambda} \sum_{\mathbf{k}} \delta(\epsilon - \xi_+ - \xi_-) \times \left[1 - \frac{1}{\xi_+ \xi_-} (a_{2,+} a_{2,-} + a_{4,+} a_{4,-}) \right], \quad (42)$$

where $a_{2,\pm} \equiv J_2 \eta s_{x,\pm} s_{y,\pm}$, $a_{3,\pm} \equiv \frac{J_1 D}{2} s_{x,\pm}$, $a_{4,\pm} \equiv J_2 \chi c_{x,\pm} c_{y,\pm}$, $a_{5,\pm} \equiv -\frac{J_1 D}{2} s_{y,\pm}$, and $\xi_\pm \equiv \sqrt{\sum_{j=2}^5 a_{j,\pm}^2}$ with the definitions $s_{\mu,\pm} \equiv \sin(k_\mu \pm \frac{q_\mu}{2})$ and $c_{\mu,\pm} \equiv \cos(k_\mu \pm \frac{q_\mu}{2})$. These susceptibilities are plotted as a func-

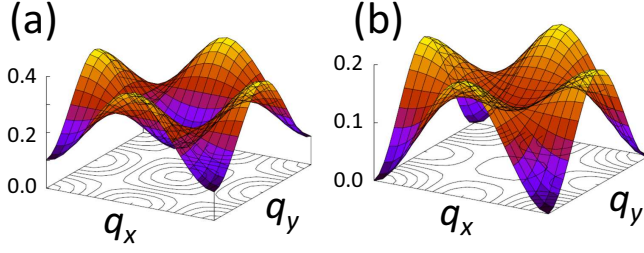


FIG. 6: Static structure factors in the mean-field approximation: (a) $C_{zz}^{(0)}(\mathbf{q}, \tau = 0)$ and (b) $C_{+-}^{(0)}(\mathbf{q}, \tau = 0)$ at $J_2 = 1.1J_1$.

tion of \mathbf{q} and ϵ in Figs. 5(a) and 5(b). As in the figure, the Hartree-Fock contributions consist only of continuum spectra, which correspond to individual spinon excitations. Since the mean-field band dispersion $\xi_{\mathbf{k}}$ of the spinon field is fully gapped [see Fig. 4(a)], the continuum spectra appear only above a critical energy, $\epsilon \geq \max_{\mathbf{k}}(\xi_+ + \xi_-)$. The frequency range of the continuum becomes broadest at $\mathbf{k} = (0, 0)$, $(\pi, 0)$, (π, π) , and $(\frac{\pi}{2}, \frac{\pi}{2})$, while narrow at $\mathbf{k} = (\pi, \frac{\pi}{2})$ and $(\frac{\pi}{2}, 0)$. This feature is because the band dispersion $\xi_{\mathbf{k}}$ has eight minima at $\mathbf{k} = (\pm\frac{\pi}{2}, 0)$, $(0, \pm\frac{\pi}{2})$, $(\pm\frac{\pi}{2}, \pi)$, and $(\pi, \pm\frac{\pi}{2})$, and eight maxima at $\mathbf{k} = (0, 0)$, $(\frac{\pi}{2}, \pm\frac{\pi}{2})$, $(-\frac{\pi}{2}, \pm\frac{\pi}{2})$, $(0, \pi)$, $(\pi, 0)$, and (π, π) [see Figs. 4(a) and 4(b)]. One should also notice that continuum in $\text{Im}\chi_{zz}^{(0)}(\mathbf{q}, \epsilon)$ has no spectral weight at $\mathbf{q} = (\pi, \pi)$, which is attributed to the staggered $U(1)$ spin-rotational symmetry given by Eq. (22).

Static spin structure factors at the mean-field level are given by the frequency integral of Eqs. (41) and (42),

$$C_{zz}^{(0)}(\mathbf{q}, \tau = 0) = \int_0^\infty d\epsilon \text{Im}\chi_{zz}^{(0)}(\mathbf{q}, \epsilon),$$

$$C_{+-}^{(0)}(\mathbf{q}, 0) = \int_0^\infty d\epsilon \text{Im}\chi_{+-}^{(0)}(\mathbf{q}, \epsilon),$$

both of which exhibit broad peak structures at $\mathbf{q} = (0, \pi)$ and $(\pi, 0)$, as shown in Fig. 6. This indicates the presence of short-range collinear antiferromagnetic correlations in the Z_2 planar state. This behavior is basically consistent with the static spin structure factor obtained in the spin nematic phase from the variational Monte Carlo calculation,²⁶ though the latter one exhibits relatively stronger collinear antiferromagnetic correlations.

B. Method of $1/N$ expansion

To capture the low-energy collective excitations, which emerge below the continuum spectra, we next include fluctuations of the auxiliary fields ($U^{\text{sin}} - \bar{U}^{\text{sin}}$ and $\mathbf{U}^{\text{tri}} - \bar{\mathbf{U}}^{\text{tri}}$) and the gauge fields ($i\mathbf{a}_\tau$) around their saddle point values. The fluctuation fields $\mathbf{r}(\mathbf{j}, \tau)$ for the Z_2 planar

state are in total given by the following 35 elements:

$$\begin{aligned} \mathbf{r}(\mathbf{j}, \tau) &\equiv (\text{Re}E_{x,3}, \text{Im}E_{x,3}, \text{Re}E_{y,3}, \text{Im}E_{y,3}, \\ &\quad \text{Re}D_{x,3}, \text{Im}D_{x,3}, \text{Re}D_{y,3}, \text{Im}D_{y,3}, \\ &\quad \text{Re}E_{x,1}, \text{Im}E_{x,1}, \text{Re}E_{y,1}, \text{Im}E_{y,1}, \\ &\quad \text{Re}D_{x,1} - D, \text{Im}D_{x,1}, \text{Re}D_{y,1}, \text{Im}D_{y,1}, \\ &\quad \text{Re}E_{x,2}, \text{Im}E_{x,2}, \text{Re}E_{y,2}, \text{Im}E_{y,2}, \\ &\quad \text{Re}D_{x,2}, \text{Im}D_{x,2}, \text{Re}D_{y,2} - D, \text{Im}D_{y,2}, \\ &\quad \text{Re}\chi_{x+y} - \chi, \text{Re}\chi_{x-y} - \chi, \text{Re}\eta_{x+y} - \eta, \text{Re}\eta_{x-y} + \eta, \\ &\quad \text{Im}\chi_{x+y}, \text{Im}\chi_{x-y}, \text{Im}\eta_{x+y}, \text{Im}\eta_{x-y}, ia_\tau^1, ia_\tau^2, ia_\tau^3). \end{aligned} \quad (43)$$

Here the vectors $\mathbf{D}_\nu = (D_{\nu,1}, D_{\nu,2}, D_{\nu,3})$ and $\mathbf{E}_\nu = (E_{\nu,1}, E_{\nu,2}, E_{\nu,3})$ with $\nu = x, y$ correspond to the vector auxiliary fields given in Eq. (7),

$$\begin{aligned} \mathbf{D}_\nu(\mathbf{j}, \tau) &= \mathbf{D}_{\mathbf{j}-\mathbf{e}_\nu/2, \mathbf{j}+\mathbf{e}_\nu/2}, \\ \mathbf{E}_\nu(\mathbf{j}, \tau) &= \mathbf{E}_{\mathbf{j}-\mathbf{e}_\nu/2, \mathbf{j}+\mathbf{e}_\nu/2}, \end{aligned}$$

where the position vector \mathbf{j} is defined on the center positions of the ferromagnetic J_1 links, whereas the fields $\chi_{x\pm y}$ and $\eta_{x\pm y}$ correspond to the scalar auxiliary fields,

$$\begin{aligned} \eta_{x\pm y}(\mathbf{j}, \tau) &= \eta_{\mathbf{j}-(\mathbf{e}_x \pm \mathbf{e}_y)/2, \mathbf{j}+(\mathbf{e}_x \pm \mathbf{e}_y)/2}, \\ \chi_{x\pm y}(\mathbf{j}, \tau) &= \chi_{\mathbf{j}-(\mathbf{e}_x \pm \mathbf{e}_y)/2, \mathbf{j}+(\mathbf{e}_x \pm \mathbf{e}_y)/2}, \end{aligned}$$

where the position \mathbf{j} is defined on the center positions of the antiferromagnetic J_2 links.

To obtain quantum corrections to the Hartree-Fock contribution [Eq. (39)], we expand the action $\mathcal{S} = \mathcal{S}_1 - \frac{1}{2N} \sum_{a=1}^N \text{Tr} \ln \mathbf{G}^{-1}$ with the small fluctuation fields $\mathbf{r}(\mathbf{j}, \tau)$ around the saddle point. Since the functional \mathbf{G}^{-1} is a linear function of the elements of h^{aa} , U^{sin} , \mathbf{U}^{tri} , and \mathbf{a}_τ , as noted below Eq. (10), the single-particle Green function takes the form

$$\begin{aligned} \mathbf{G}_{(\mathbf{k}, n, a | \mathbf{k}', n', a)}^{-1} &= \mathbf{G}_{0, (\mathbf{k}, n, a | \mathbf{k}', n', a)}^{-1} \\ &+ \frac{1}{\sqrt{\beta N_\Lambda}} \sum_{\mathbf{q}} \sum_m \delta_{\mathbf{k}, \mathbf{k}'+\mathbf{q}} \delta_{n, n'+m} r_\alpha(\mathbf{q}, m) \mathbf{v}_\alpha(\mathbf{k}, \mathbf{k}'), \end{aligned} \quad (44)$$

where the bosonic fluctuation fields \mathbf{r} are transformed as

$$r_\alpha(\mathbf{q}, m) \equiv \frac{1}{\sqrt{\beta N_\Lambda}} \sum_{\mathbf{j}} \int_0^\beta d\tau e^{-i\mathbf{j} \cdot \mathbf{q} - i\epsilon_m \tau} r_\alpha(\mathbf{j}, \tau).$$

Here, the index α ($\alpha = 1, \dots, 35$) specifies the element of the fluctuation fields enumerated in Eq. (43), and the summation of the position vector \mathbf{j} runs over all the center positions of nearest neighbor links for $\alpha = 1, \dots, 24$, all the center positions of second nearest neighbor links for $\alpha = 25, \dots, 32$, and all the lattice sites for $\alpha = 33, 34, 35$. The summation over the repeated index α is made implicit and will be so henceforth. In

the same sequence as in Eq. (43), the internal vertices \mathbf{v}_α are explicitly given by the 4×4 matrix forms

$$\begin{aligned} \mathbf{v}(\mathbf{k}, \mathbf{k}') &\equiv \begin{pmatrix} -\bar{c}_x \gamma_{35}, -\bar{s}_x \gamma_{12}, -\bar{c}_y \gamma_{35}, -\bar{s}_y \gamma_{12}, \\ \bar{s}_x \gamma_1, \bar{s}_x \gamma_{14}, \bar{s}_y \gamma_1, \bar{s}_y \gamma_{14}, \\ -\bar{c}_x \gamma_{15}, -\bar{s}_x \gamma_{23}, -\bar{c}_y \gamma_{15}, -\bar{s}_y \gamma_{23}, \\ -\bar{s}_x \gamma_3, -\bar{s}_x \gamma_{34}, -\bar{s}_y \gamma_3, -\bar{s}_y \gamma_{34}, \\ \bar{c}_x \gamma_{31}, \bar{s}_x \gamma_{25}, \bar{c}_y \gamma_{31}, \bar{s}_y \gamma_{25}, \\ \bar{s}_x \gamma_5, -\bar{s}_x \gamma_{45}, \bar{s}_y \gamma_5, -\bar{s}_y \gamma_{45}, \\ -\bar{c}'_{x+y} \gamma_4, -\bar{c}'_{x-y} \gamma_4, \bar{c}'_{x+y} \gamma_2, \bar{c}'_{x-y} \gamma_2, \\ -\bar{s}'_{x+y} \gamma_0, -\bar{s}'_{x-y} \gamma_0, \bar{c}'_{x+y} \gamma_{24}, \bar{c}'_{x-y} \gamma_{24}, -\gamma_2, \gamma_{24}, \gamma_4 \end{pmatrix}, \end{aligned} \quad (45)$$

where

$$\begin{aligned} \bar{c}_\mu &= \frac{J_1}{2} \cos\left(\frac{k_\mu + k'_\mu}{2}\right), \\ \bar{s}_\mu &= \frac{J_1}{2} \sin\left(\frac{k_\mu + k'_\mu}{2}\right), \\ \bar{c}'_{x\pm y} &= \frac{J_2}{2} \cos\left(\frac{k_x + k'_x \pm k_y \pm k'_y}{2}\right), \\ \bar{s}'_{x\pm y} &= \frac{J_2}{2} \sin\left(\frac{k_x + k'_x \pm k_y \pm k'_y}{2}\right). \end{aligned}$$

Using the expression of Eq. (44), we obtain a series expansion of the action with the fluctuation fields \mathbf{r} around the saddle point,

$$\begin{aligned} \mathcal{S} &= \mathcal{S}_I - \frac{1}{2N} \sum_{a=1}^N \text{Tr} \ln \mathbf{G}^{-1} \\ &= \mathcal{S}^{(0)} + \mathcal{S}_\alpha^{(1)} r_\alpha + \mathcal{S}_{\alpha,\alpha'}^{(2)} r_\alpha r_{\alpha'} \\ &\quad + \sum_{n=3}^{\infty} \mathcal{S}_{\alpha_1, \alpha_2, \dots, \alpha_n}^{(n)} r_{\alpha_1} r_{\alpha_2} \cdots r_{\alpha_n}, \end{aligned} \quad (46)$$

where the coefficients $\mathcal{S}_{\alpha_1, \alpha_2, \dots, \alpha_n}^{(n)}$ are given by

$$\begin{aligned} \mathcal{S}_{\alpha_1, \alpha_2, \dots, \alpha_n}^{(n)} &= \frac{1}{n!} \frac{\partial^n \mathcal{S}}{\partial r_{\alpha_1} \cdots \partial r_{\alpha_n}} \Big|_{\mathbf{r}=0} \\ &= \frac{\partial \mathcal{S}_I}{\partial r_{\alpha_1}} \Big|_{\mathbf{r}=0} \delta_{n,1} + \frac{1}{2} \frac{\partial^2 \mathcal{S}_I}{\partial r_{\alpha_1} \partial r_{\alpha_2}} \Big|_{\mathbf{r}=0} \delta_{n,2} \\ &\quad + \frac{(-1)^n}{2Nn(\beta N_\Lambda)^{n/2}} \sum_{a=1}^N \text{Tr} [\mathbf{G}_0 \mathbf{v}_{\alpha_1} \mathbf{G}_0 \mathbf{v}_{\alpha_2} \cdots \mathbf{G}_0 \mathbf{v}_{\alpha_n}] \end{aligned} \quad (47)$$

for $n \geq 1$. The trace here is taken over the momentum, Matsubara frequency, spin, and particle-hole indices. The summation of the flavor index is written explicitly. One finds that all the coefficients $\mathcal{S}_{\alpha_1, \alpha_2, \dots, \alpha_n}^{(n)}$ are of order $O(1)$ in the large N limit. Note that \mathbf{v}_α plays a role of an internal vertex which connects two Green functions with the fluctuation field r_α .

To calculate the correlation functions Eqs. (37) and (38), we further perform a series expansion of the action

(46) in the small field h^{aa} . We only need the series of $\{h_\mu^{aa}\}$ with a certain flavor a ,

$$\begin{aligned} \mathcal{S} &= \bar{\mathcal{S}}^{(0,0)} + \bar{\mathcal{S}}_{\alpha, \alpha'}^{(0,2)} r_\alpha r_{\alpha'} + \sum_{n=3}^{\infty} \bar{\mathcal{S}}_{\alpha_1, \alpha_2, \dots, \alpha_n}^{(0,n)} r_{\alpha_1} r_{\alpha_2} \cdots r_{\alpha_n} \\ &\quad + \frac{1}{N} \sum_{\mu=1}^3 \sum_{n=1}^{\infty} \bar{\mathcal{S}}_{\mu; \alpha_1, \dots, \alpha_n}^{(1,n)} r_{\alpha_1} \cdots r_{\alpha_n} h_\mu^{aa} \\ &\quad + \frac{1}{N} \sum_{\mu, \nu=1}^3 \sum_{n=0}^{\infty} \bar{\mathcal{S}}_{\mu, \nu; \alpha_1, \dots, \alpha_n}^{(2,n)} r_{\alpha_1} \cdots r_{\alpha_n} h_\mu^{aa} h_\nu^{aa}, \end{aligned} \quad (48)$$

where

$$\bar{\mathcal{S}}_{\alpha_1, \dots, \alpha_n}^{(0,n)} \equiv \mathcal{S}_{\alpha_1, \dots, \alpha_n}^{(n)} \Big|_{h=0}, \quad (49)$$

$$\bar{\mathcal{S}}_{\mu; \alpha_1, \dots, \alpha_n}^{(1,n)} \equiv N \frac{\partial \mathcal{S}_{\alpha_1, \dots, \alpha_n}^{(n)}}{\partial h_\mu^{aa}} \Big|_{h=0}, \quad (50)$$

$$\bar{\mathcal{S}}_{\mu, \nu; \alpha_1, \dots, \alpha_n}^{(2,n)} \equiv \frac{N}{2} \frac{\partial^2 \mathcal{S}_{\alpha_1, \dots, \alpha_n}^{(n)}}{\partial h_\mu^{aa} \partial h_\nu^{aa}} \Big|_{h=0} \quad (51)$$

with $n \geq 0$ and with the definition $\mathcal{S}_{\alpha_1, \dots, \alpha_n}^{(n)} = \mathcal{S}^{(0)}$ if $n = 0$. Equation (48) does not have any linear term in \mathbf{r} , by definition of the saddle point, and any linear term in h_μ^{aa} , as $\bar{\mathcal{S}}_{\mu}^{(1,0)} \sim \sum_{k,n} \text{Tr}[g_0(k, i\omega_n) \mathbf{u}_\mu] = 0$. The coefficient $\bar{\mathcal{S}}_{\mu, \nu}^{(2,0)}$ corresponds to Hartree-Fock susceptibility $\bar{\mathcal{S}}_{\mu, \nu}^{(2,0)} = -\chi_{\mu\nu}^{aa,(0)}/2$. Note that the coefficients $\bar{\mathcal{S}}_{\mu; \alpha_1, \dots, \alpha_n}^{(1,n)}$ and $\bar{\mathcal{S}}_{\mu, \nu; \alpha_1, \dots, \alpha_n}^{(2,n)}$ are functions of order unity in the large N limit. This is because $N\mathcal{S}^{(n)}$ is composed by a summation over the flavor indices and the field derivative, selecting the index a , leads to a result of order unity. All coefficients $\bar{\mathcal{S}}_{\alpha_1, \dots, \alpha_n}^{(0,n)}$, $\bar{\mathcal{S}}_{\mu; \alpha_1, \dots, \alpha_n}^{(1,n)}$, and $\bar{\mathcal{S}}_{\mu, \nu; \alpha_1, \dots, \alpha_n}^{(2,n)}$ are order $O(1)$ in the large- N limit.

We regard the quadratic term in \mathbf{r} as a non-perturbed Gaussian action for the fluctuation fields and treat the rest of terms as perturbations. The coefficient of the quadratic term corresponds to the fluctuation-field propagator

$$\frac{1}{N} \left[\left(\bar{\mathcal{S}}^{(0,2)} \right)^{-1} \right]_{\alpha_1, \alpha_2} = \frac{\int d\mathbf{r} r_{\alpha_1} r_{\alpha_2} \exp \left[-N \bar{\mathcal{S}}_{\alpha, \alpha'}^{(0,2)} r_\alpha r_{\alpha'} \right]}{\int d\mathbf{r} \exp \left[-N \bar{\mathcal{S}}_{\alpha, \alpha'}^{(0,2)} r_\alpha r_{\alpha'} \right]}, \quad (52)$$

which is given by Eq. (47) as

$$\bar{\mathcal{S}}_{\alpha, \alpha'}^{(0,2)} = \frac{1}{2} \frac{\partial^2 \mathcal{S}_I}{\partial r_\alpha \partial r_{\alpha'}} \Big|_{\mathbf{r}=0, h=0} + \frac{1}{4\beta N_\Lambda} \sum_{k,n} \text{Tr} [g_0 \mathbf{v}_\alpha g_0 \mathbf{v}_{\alpha'}]. \quad (53)$$

In the perturbation terms of Eq. (48), each internal vertex \mathbf{v}_α is connected with two single-particle Green Functions (solid lines) and one fluctuation field (wavy line), and each external vertex \mathbf{u}_μ is with two single-particle Green Functions and one external magnetic field

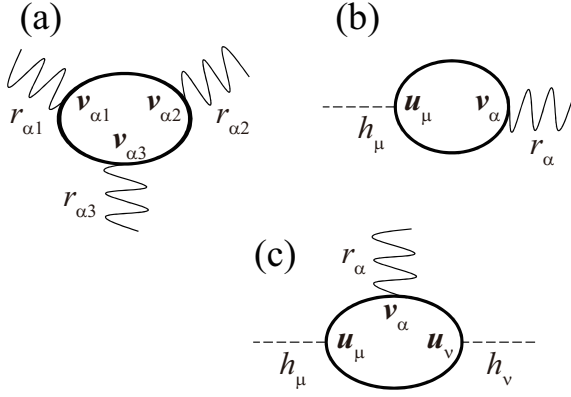


FIG. 7: Diagrams of interactions in Eq. (48) containing the renormalized vertex parts (a) $\overline{\mathcal{S}}^{(0,3)}$, (b) $\overline{\mathcal{S}}^{(1,1)}$, and (c) $\overline{\mathcal{S}}^{(2,1)}$.

(dashed line), as shown in Fig. 7. The interactions containing $\overline{\mathcal{S}}^{(0,n)}$ (with $n > 2$), $\overline{\mathcal{S}}^{(1,n)}$, and $\overline{\mathcal{S}}^{(2,n)}$ have single

loops composed by multiple one-particle Green functions and vertices. See for example Figs. 7(a)–(c). Symbolically, $\overline{\mathcal{S}}^{(1,1)}$ and $\overline{\mathcal{S}}^{(2,1)}$ take the following forms

$$\overline{\mathcal{S}}_{\mu;\alpha}^{(1,1)} = \frac{1}{4\beta N_{\Lambda}} \sum_{k,i\omega_n} \text{Tr}[g_0 \mathbf{u}_{\mu} g_0 \mathbf{v}_{\alpha}], \quad (54)$$

$$\overline{\mathcal{S}}_{\mu,\nu;\alpha}^{(2,1)} = -\frac{1}{16(\beta N_{\Lambda})^{3/2}} \sum_{k,i\omega_n} \left\{ \text{Tr}[g_0 \mathbf{u}_{\nu} g_0 \mathbf{u}_{\mu} g_0 \mathbf{v}_{\alpha}] + \text{Tr}[g_0 \mathbf{u}_{\mu} g_0 \mathbf{u}_{\nu} g_0 \mathbf{v}_{\alpha}] \right\}, \quad (55)$$

where \mathbf{k} and $i\omega_n$ denote the momentum and the frequency inside of the loops. The traces in Eqs. (53)–(55) are only over the particle-hole and spin indices but not over the flavor index.

Using the series (48), we can expand the spin correlation functions $\chi_{\mu\nu}^{aa} \equiv \chi_{\mu\nu,\text{I}}^{aa} + \chi_{\mu\nu,\text{II}}^{aa}$ as²⁹

$$\chi_{\mu\nu,\text{I}}^{aa}(\mathbf{q}, i\epsilon_n) = -\frac{1}{Z} \int \mathcal{D}\mathbf{r} \left(\sum_{n=0}^{\infty} \overline{\mathcal{S}}_{\mu,\nu;\alpha_1,\dots,\alpha_n}^{(2,n)} r_{\alpha_1} \cdots r_{\alpha_n} \right) \sum_{m=0}^{\infty} \frac{(-N)^m}{m!} \left(\sum_{l=3}^{\infty} \overline{\mathcal{S}}_{\alpha_1,\dots,\alpha_l}^{(0,l)} r_{\alpha_1} \cdots r_{\alpha_l} \right)^m e^{-N \overline{\mathcal{S}}_{\alpha,\alpha'}^{(0,2)} r_{\alpha} r_{\alpha'}}, \quad (56)$$

$$\begin{aligned} \chi_{\mu\nu,\text{II}}^{aa}(\mathbf{q}, i\epsilon_n) = & \frac{1}{Z} \int \mathcal{D}\mathbf{r} \left(\sum_{n=1}^{\infty} \overline{\mathcal{S}}_{\mu;\alpha_1,\dots,\alpha_n}^{(1,n)} r_{\alpha_1} \cdots r_{\alpha_n} \right) \left(\sum_{l=1}^{\infty} \overline{\mathcal{S}}_{\nu;\alpha_1,\dots,\alpha_l}^{(1,l)} r_{\alpha_1} \cdots r_{\alpha_l} \right) \\ & \times \sum_{m=0}^{\infty} \frac{(-N)^m}{m!} \left(\sum_{j=3}^{\infty} \overline{\mathcal{S}}_{\alpha_1,\dots,\alpha_j}^{(0,j)} r_{\alpha_1} \cdots r_{\alpha_j} \right)^m e^{-N \overline{\mathcal{S}}_{\alpha,\alpha'}^{(0,2)} r_{\alpha} r_{\alpha'}}, \end{aligned} \quad (57)$$

where $\overline{\mathcal{S}}^{(0,0)}$ was omitted. The Gaussian integrals over the real-valued fields \mathbf{r} can be taken, reducing even numbers of the fields to a sum over all the possible pairwise contractions among the fields;

$$\int \mathcal{D}\mathbf{r} r_1 \cdots r_{2k} \exp[-N \overline{\mathcal{S}}_{\alpha,\alpha'}^{(0,2)} r_{\alpha} r_{\alpha'}] = \sum_{\sigma} \frac{1}{N^k} [\overline{\mathcal{S}}^{(0,2),-1}]_{\sigma(1),\sigma(2)} [\overline{\mathcal{S}}^{(0,2),-1}]_{\sigma(3),\sigma(4)} \cdots [\overline{\mathcal{S}}^{(0,2),-1}]_{\sigma(2k-1),\sigma(2k)}. \quad (58)$$

The summation over σ runs over the arbitrary permutations among the $2k$ indices.

We can evaluate the N dependence of each term in Eqs. (56) and (57), using the facts that all coefficients $\overline{\mathcal{S}}_{\alpha_1,\dots,\alpha_n}^{(0,n)}$, $\overline{\mathcal{S}}_{\mu;\alpha_1,\dots,\alpha_n}^{(1,n)}$, and $\overline{\mathcal{S}}_{\mu,\nu;\alpha_1,\dots,\alpha_n}^{(2,n)}$ are of order unity and one Gaussian integral of a pair of fluctuation fields leads to one prefactor $1/N$ [see Eq. (58)]. In Eq. (56), the term with the summation indices (l, m, n) is of order $O(N^{-n/2-(l-2)m/2})$. In Eq. (57), the term with the summation indices (l, m, n, j) is of order $O(N^{-n/2-l/2-m(j-2)/2})$. These order estimates give a controlled expansion of physical quantities with a small parameter $1/N$.

To enumerate all the contractions possible in Eqs. (56) and (57), we use Feynman diagrams. Connecting one internal vertex \mathbf{v}_{α} with another one \mathbf{v}_{β} by a wavy

line, which represents the fluctuation-field propagator $[\overline{\mathcal{S}}^{(0,2),-1}]_{\alpha,\beta}$, we obtain all possible diagrams. As an example, we depict all diagrams of spin correlation functions of order $O(1/N)$ in Fig. 8, where those diagrams which vanish by themselves have been already omitted.

C. Next-to-leading order corrections to the correlation functions

From the order estimation explained in Sec. III B, the leading order contribution to the spin correlation function is the Hartree-Fock solution, Eq. (40), which is order unity. The next-to-leading order corrections of order $O(1/N)$ in the $1/N$ expansion are given by the Feynman diagrams depicted in Fig. 8.

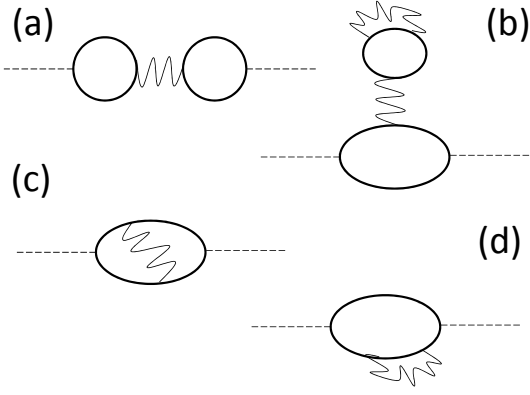


FIG. 8: $1/N$ -contributions to correlation functions, where dotted lines denote external fields, wavy lines are the RPA propagators, and solid lines are single-particle Green functions. Diagram (a) contributes to $\chi_{\mu\mu,\Pi}^{aa}(q, i\epsilon_n)$, while diagrams (b,c,d) to $\chi_{\mu\mu,\Pi}^{aa}(q, i\epsilon_n)$. They contribute to (a) spin-wave term, (b,d) Hartree-Fock (HF) term with renormalized single-particle Green functions, and (c) HF term with a vertex correction.

Among these diagrams, only the diagram Fig. 8(a) endows the imaginary part of the dynamical spin susceptibilities with finite spectral weight due to the low-energy collective modes. Figs. 8(b)–(d) take the same structure as that of the mean-field diagram Fig. 5(d). The difference can be solely attributed to a proper renormalization of the single-particle Green function in the cases (b) and (d), and a renormalization of the external vertex in the case (c). Thus, their major contribution is more or less modification of shape and intensity of the Stoner continuum, which already appears in the leading order. In Fig. 8(a), on the other hand, the momentum and energy carried by one of the external lines are transmitted to the other only through the fluctuation-field propagator, namely RPA propagator, into which various collective excitations including gapless Goldstone modes and gapped ‘gauge-field’ like collective modes are encoded. As a result, some of low-energy poles of the RPA propagator show up as coherent bosonic peaks in the imaginary part of susceptibilities given by Fig. 8(a).

We henceforth focus on Fig. 8(a) to discuss low-energy collective modes. We will see that these collective modes directly come from the poles in the RPA propagators which connect two loops of single-particle Green functions. To derive its expression, let us first clarify possible low-energy poles encoded in the RPA propagator. The RPA propagator defined in Eq. (53) is always a block-diagonal matrix with respect to the following four groups

of fluctuation fields:

$$\mathbf{R}_1 \equiv \text{Re}D_{y,3} \mathbf{e}_1^1 + \text{Im}D_{x,3} \mathbf{e}_2^1 + \text{Im}E_{x,3} \mathbf{e}_3^1 + \text{Re}E_{y,3} \mathbf{e}_4^1, \quad (59)$$

$$\mathbf{R}_2 \equiv \text{Re}D_{x,3} \mathbf{e}_1^2 + \text{Im}D_{y,3} \mathbf{e}_2^2 + \text{Im}E_{y,3} \mathbf{e}_3^2 + \text{Re}E_{x,3} \mathbf{e}_4^2, \quad (60)$$

$$\begin{aligned} \mathbf{R}_3 \equiv & \text{Re}D_{x,2} \mathbf{e}_1^3 + \text{Re}D_{y,1} \mathbf{e}_2^3 + \text{Im}D_{y,2} \mathbf{e}_3^3 \\ & + \text{Im}D_{x,1} \mathbf{e}_4^3 + \text{Im}E_{y,2} \mathbf{e}_5^3 + \text{Im}E_{x,1} \mathbf{e}_6^3 \\ & + \text{Re}E_{x,2} \mathbf{e}_7^3 + \text{Re}E_{y,1} \mathbf{e}_8^3 + \frac{\text{Im}\chi_{x+y} + \text{Im}\chi_{x-y}}{\sqrt{2}} \mathbf{e}_9^3 \\ & + \frac{\text{Im}\eta_{x+y} + \text{Im}\eta_{x-y}}{\sqrt{2}} \mathbf{e}_{10}^3 + \frac{\text{Im}\chi_{x+y} - \text{Im}\chi_{x-y}}{\sqrt{2}} \mathbf{e}_{11}^3 \\ & + \frac{\text{Im}\eta_{x+y} - \text{Im}\eta_{x-y}}{\sqrt{2}} \mathbf{e}_{12}^3 + ia_\tau^3 \mathbf{e}_{13}^3 + ia_\tau^1 \mathbf{e}_{14}^3, \end{aligned} \quad (61)$$

$$\begin{aligned} \mathbf{R}_4 \equiv & (\text{Re}D_{x,1} - D) \mathbf{e}_1^4 + (\text{Re}D_{y,2} - D) \mathbf{e}_2^4 \\ & + \text{Im}D_{y,1} \mathbf{e}_3^4 + \text{Im}D_{x,2} \mathbf{e}_4^4 + \text{Im}E_{y,1} \mathbf{e}_5^4 \\ & + \text{Im}E_{x,2} \mathbf{e}_6^4 + \text{Re}E_{x,1} \mathbf{e}_7^4 + \text{Re}E_{y,2} \mathbf{e}_8^4 \\ & + (\text{Re}\chi_{x+y} - \chi) \mathbf{e}_9^4 + (\text{Re}\eta_{x+y} - \eta) \mathbf{e}_{10}^4 \\ & + (\text{Re}\chi_{x+y} - \chi) \mathbf{e}_{11}^4 + (\text{Re}\eta_{x+y} + \eta) \mathbf{e}_{12}^4 + ia_\tau^2 \mathbf{e}_{13}^4, \end{aligned} \quad (62)$$

where $\{\mathbf{e}_\alpha^\mu\}$ denotes the orthonormal basis of 35-dimensional space \mathbb{R}^{35} and the renamed fluctuation fields $\{R_{\mu,\alpha}\}$ are defined through $\mathbf{R}_\mu = \sum_\alpha R_{\mu,\alpha} \mathbf{e}_\alpha^\mu$. In this definition, for example, the coefficient of the base \mathbf{e}_1^1 corresponds to the 7-th component of \mathbf{r} [see Eq. (43)]. Using this representation, the Gaussian part of the action is indeed decomposed into four parts,

$$\left[\bar{\mathcal{S}}^{(0,2)}\right]_{\alpha,\beta} r_\alpha r_\beta = \sum_{\mu=1}^4 \left[\bar{\mathcal{S}}_{\mu\mu}^{(0,2)}\right]_{\alpha,\beta} R_{\mu,\alpha} R_{\mu,\beta}, \quad (63)$$

where the matrix elements inside of each block are given by

$$\begin{aligned} \left[\bar{\mathcal{S}}_{\mu\mu}^{(0,2)}(\mathbf{q}, i\epsilon_n)\right]_{\alpha,\beta} \equiv & \frac{1}{2} \frac{\partial^2 \mathcal{S}_1}{\partial r_{\mu,\alpha} \partial r_{\mu,\beta}} + \frac{1}{4\beta N_\Lambda} \sum_{\mathbf{k},n} \\ & \times \text{Tr}[\mathbf{g}_0(\mathbf{k} + \mathbf{q}, i\omega_n + i\epsilon_n) \mathbf{v}_{\mu,\beta} \mathbf{g}_0(\mathbf{k}, i\omega_n) \mathbf{v}_{\mu,\alpha}] \end{aligned} \quad (64)$$

in the momentum representation. The internal vertices here are also defined so that $\sum_{\alpha=1}^{35} r_\alpha \mathbf{v}_\alpha = \sum_{\mu=1}^4 \sum_\alpha R_{\mu,\alpha} \mathbf{v}_{\mu,\alpha}$. Explicit expressions for $[\bar{\mathcal{S}}_{\mu\mu}^{(0,2)}]_{\alpha,\beta}$ are given in Appendix [Eqs.(A1)–(A92)].

One can also see that, in the vertices $\bar{\mathcal{S}}_{\mu;\alpha}^{(1,1)} h_\mu r_\alpha$, the fluctuation fields in \mathbf{R}_μ with $\mu = 1, 2, 3$ are, respectively, coupled only with the μ -th components of the external magnetic field, h_μ , in the form

$$\bar{\mathcal{S}}_{\mu;\alpha}^{(1,1)} h_\mu r_\alpha = \sum_{\mu=1}^3 \left[\bar{\mathcal{S}}_{\mu;\mu}^{(1,1)}\right]_\alpha h_\mu R_{\mu,\alpha}, \quad (65)$$

where

$$\begin{aligned} \left[\bar{\mathcal{S}}_{\mu;\mu}^{(1,1)}(\mathbf{q}, i\epsilon_n) \right]_{\alpha} &\equiv \frac{1}{4\beta N_{\Lambda}} \sum_{\mathbf{k}, n} \\ &\times \text{Tr}[\mathbf{g}_0(\mathbf{k} + \mathbf{q}, i\omega_n + i\epsilon_n) \mathbf{u}_{\mu} \mathbf{g}_0(\mathbf{k}, i\omega_n) \mathbf{v}_{\mu, \alpha}], \quad (66) \end{aligned}$$

while all fluctuation fields enumerated in \mathbf{R}_4 are discon-

nected from the external magnetic fields. Explicit expressions for $\bar{\mathcal{S}}_{\mu;\alpha}^{(1,1)}$ ($\mu = 1, 2, 3$) are given in the Appendix [Eqs.(A93)–(A109)].

Using Eqs. (64) and (66), we finally obtain the contribution from Fig. 8(a) as

$$\chi_{\mu\mu, \Pi}^{(1)}(\mathbf{q}, i\epsilon_n) = \left[\bar{\mathcal{S}}_{\mu;\mu}^{(1,1)}(\mathbf{q}, i\epsilon_n) \right]_{\alpha} \left[\left(\bar{\mathcal{S}}_{\mu\mu}^{(0,2)}(\mathbf{q}, i\epsilon_n) \right)^{-1} \right]_{\alpha, \beta} \left[\bar{\mathcal{S}}_{\mu;\mu}^{(1,1)}(-\mathbf{q}, -i\epsilon_n) \right]_{\beta}. \quad (67)$$

Here, the vertex parts do not give rise to any finite contribution to $\text{Im}\chi^{(1)}(\mathbf{q}, \epsilon + i\delta)$ below the Stoner continuum, i.e., for $|\epsilon| < \min_{\mathbf{k}}(\xi_{\mathbf{k}+\mathbf{q}} + \xi_{\mathbf{k}})$. This is because Eq. (66) has the same structure as the Hartree-Fock contribution, the first term in Eq. (40), and it always has the form

$$\left[\bar{\mathcal{S}}_{\mu;\mu}^{(1,1)}(\mathbf{q}, \epsilon) \right]_{\alpha} = \sum_{\mathbf{k}} \frac{A_{\mathbf{k}, \mathbf{q}, \alpha}(\epsilon)}{-\epsilon^2 + (\xi_{\mathbf{k}+\mathbf{q}} + \xi_{\mathbf{k}})^2} \quad (68)$$

for any μ and α , where the numerator is a regular function of ϵ with $[\bar{\mathcal{S}}_{\mu;\mu}^{(1,1)}(-\mathbf{q}, -\epsilon)]_{\alpha} = [\bar{\mathcal{S}}_{\mu;\mu}^{(1,1)}(\mathbf{q}, \epsilon)]_{\alpha}^*$ [see Eqs. (A88), (A89), and (A94)–(A109)]. Hence, we can attribute any finite spectral weight in $\text{Im}\chi_{\mu\mu, \Pi}^{(1)}(\mathbf{q}, \epsilon)$ below the Stoner continuum solely to the poles in the RPA propagator, i.e., the zeros of the eigenvalues of Eq. (64).

Before moving to the discussions of obtained dynamical spin susceptibilities, we briefly mention about unphysical zero modes which are encoded in the Gaussian action, i.e., RPA propagator Eq. (64). The Gaussian part in the static limit ($i\epsilon_n = 0$) always has three zero modes at *arbitrary* \mathbf{q} , which comes from the $SU(2)$ local gauge symmetry⁹

$$\Psi_j^{\dagger} \rightarrow \Psi_j^{\dagger} e^{i\phi_j \sigma_{\mu}}, \quad \Psi_j \rightarrow e^{-i\phi_j \sigma_{\mu}} \Psi_j \quad (69)$$

with $\mu = 1, 2, 3$. Two zero modes with $\mu = 1$ and 3 belong to \mathbf{R}_3 , while the other ($\mu = 2$) belongs to \mathbf{R}_4 . However, these excitations do not change the ground state itself; all mean-field ansatzes which are transformed to one another by the local gauge symmetry should be regarded as an identical state. Clearly, none of these modes couple with external magnetic fields at any \mathbf{q} . We hence regard these three zero modes as unphysical modes. For example, the gauge transformation with $\phi_j = (-1)^{j_x + j_y}$ for $\mu = 3$ requires that \mathbf{e}_{12}^3 -fluctuation becomes a zero mode at $\mathbf{q} = (\pi, \pi)$ in the Z_2 planar phase. From Eq. (A93), one finds that the coupling to the field vanishes as $[\mathcal{S}_{3,3}^{(1,1)}]_{12} h_3 R_{3,12} = 0$.

IV. DYNAMICAL STRUCTURE FACTORS

In this section, we discuss the dynamical spin structure factors $\text{Im}\chi_{\mu\mu}(\mathbf{q}, \epsilon)$ in spin nematic ground states obtained from the $1/N$ expansion up to first order in $1/N$. To find the nature of collective modes, we analyze the next-to-leading order terms, especially $\text{Im}\chi_{\mu\mu, \Pi}^{(1)}(\mathbf{q}, \epsilon)$, at zero temperature given by Eq. (67). For simplicity, the fluctuations of the temporal gauge fields, ia_{τ}^{μ} ($\mu = 1, 2, 3$), are not included in these calculations, so that collective excitations are comprised only of the fluctuations of auxiliary fields. Following a standard convention, we denote the quantity $\text{Im}\chi_{33}(\mathbf{q}, \epsilon)$ by $\text{Im}\chi_{zz}(\mathbf{q}, \epsilon)$ and $\text{Im}\chi_{11}(\mathbf{q}, \epsilon)$ by $\text{Im}\chi_{xx}(\mathbf{q}, \epsilon)$ hereafter.

In the first two subsections (Secs. IV A and IV B), we describe the characters of low-energy collective modes and associated spectral weight of the dynamical spin structure factors in the Z_2 planar phase. Typical numerical plots of $\text{Im}\chi_{zz}(\mathbf{q}, \epsilon)$ and $\text{Im}\chi_{+-}(\mathbf{q}, \epsilon)$ are shown in Figs. 9 and 10 respectively for the parameter point $J_2/J_1 = 1.1$. We focus on the collective modes in the vicinity of symmetric momentum points $\mathbf{q} = (0, 0)$, $(\pi, 0)$, and (π, π) . At Γ point [$\mathbf{q} = (0, 0)$], we find three gapless q -linear collective modes and also gapful modes. These gapless modes are associated with director-wave excitations, which are accompanied by weak spin excitations.

In Sec. IV C, we discuss the nature of excitations when the coupling ratio J_2/J_1 is changed to $J_2/J_1 = J_{c,2}$, i.e., the boundary to the neighboring $U(1)$ planar phase. We find that two gapped modes in $\text{Im}\chi_{zz}(\mathbf{q}, \epsilon)$ at $\mathbf{q} = (\pi, \pi)$ become gapless (see Fig. 12), which corresponds to the appearance of gapless gauge excitations ('photon-like' excitation) in the $U(1)$ phase. We also argue the appearance of a new instability to a certain space symmetry breaking in the $U(1)$ planar phase.

A. Near Γ -point

Since the Z_2 planar state breaks all the spin-rotational symmetries, there are three gapless Nambu-Goldstone modes at the Γ -point corresponding to the

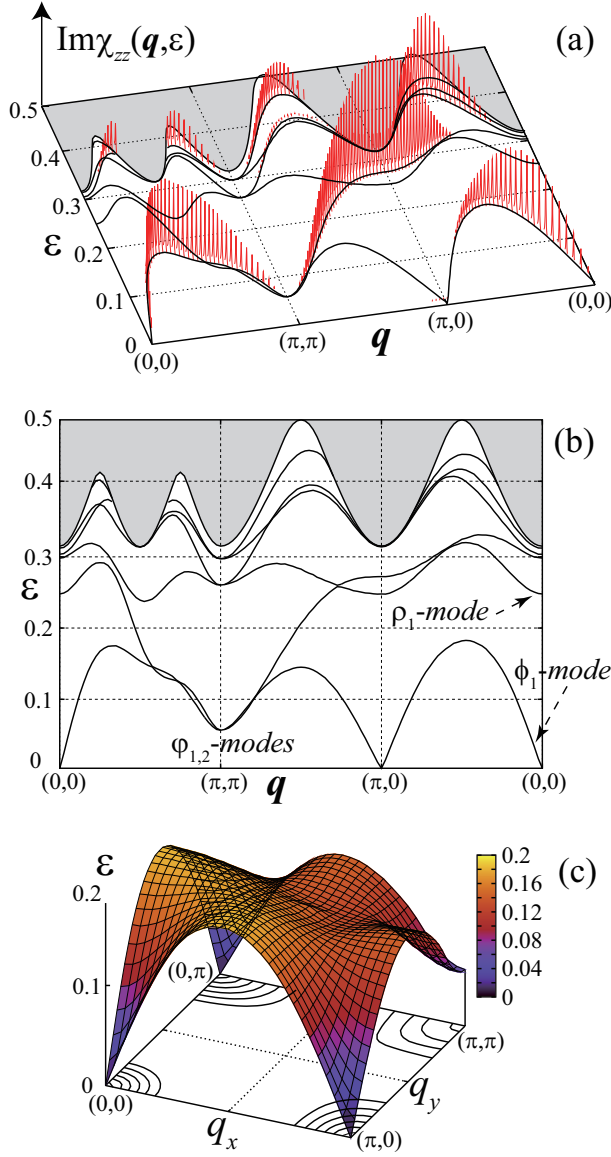


FIG. 9: (Color online) Excitation energy spectrum in the dynamical structure factor $\text{Im}\chi_{zz}(\mathbf{q}, \epsilon)$ in the Z_2 planar ground state at $J_2/J_1 = 1.1$. (a) Spectral weight of the collective modes. (b) Momentum-energy dispersion relation, showing the characteristic collective modes (ϕ_1 , φ_1 , φ_2 , ρ_1) given in the text. The momentum runs along three high symmetric q -points [see Fig. 5(c)]. The grey zones denote Stoner continuum. (c) Momentum-energy dispersion relation for the lowest collective modes in the first quadrant of the Brillouin zone.

long-wavelength director-wave excitations. The eigenmodes of the corresponding fluctuation fields take the following forms at $\mathbf{q} = (0, 0)$:

$$\phi_1 \equiv \frac{1}{\sqrt{2}}(\mathbf{e}_1^3 - \mathbf{e}_2^3), \quad \phi_2 \equiv \mathbf{e}_1^1, \quad \phi_3 \equiv \mathbf{e}_2^2. \quad (70)$$

The ϕ_1 -mode and $\phi_{2,3}$ -modes appear, respectively, as the gapless excitations in $\text{Im}\chi_{zz}(\mathbf{q}, \epsilon)$ and $\text{Im}\chi_{+-}(\mathbf{q}, \epsilon)$ (see Figs. 9 and 10). These eigenmodes induce global

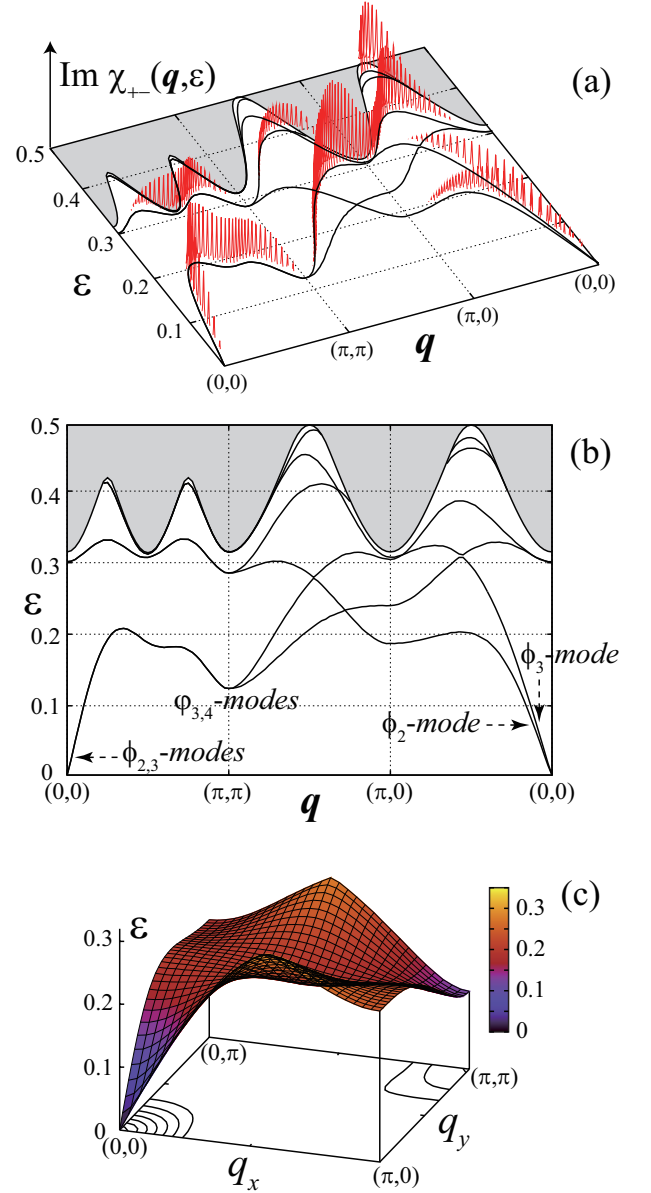


FIG. 10: (Color online) Excitation energy spectrum in the dynamical structure factor $\text{Im}\chi_{+-}(\mathbf{q}, \epsilon)$ in the Z_2 planar ground state at $J_2/J_1 = 1.1$. (a) Spectral weight of the collective modes. (b) Momentum-energy dispersion relations, showing the collective modes (ϕ_2 , ϕ_3 , φ_3 , φ_4) given in the text. The grey zones denote Stoner continuum. (c) Momentum-energy dispersion relation for the lowest collective modes in the first quadrant of the Brillouin zone.

rotations of nematic directors. The gapless mode ϕ_1 corresponds to a director rotation about spin 3-axis, which is generated by $\sum_j S_{j,3}^{aa}$. The other two gapless modes ϕ_2 and ϕ_3 , respectively, correspond to director rotations about spin 1- and 2-axes, given by the generators $\sum_j S_{j,\mu}^{aa}$ with $\mu = 1$ and 2. These assignments of the nature of gapless excitations are consistent with the semi-classical argument given in Ref. 9. Under the mirror reflection

which exchanges both the spin 1 and 2 axes and the space x and y axes, the planar state is symmetric, and the ϕ_2 - and ϕ_3 -modes are interchanged. Thus, these two modes are energetically degenerate along the line from $(0, 0)$ to (π, π) , while the degeneracy is lifted away from this symmetric line (see Fig. 10).

In a finite-momentum regime of these gapless branches, spin-wave excitations are also induced together with director-wave excitations. We can see that a fluctuation field $R_{3,1}\phi_1$ (we set $R_{3,2} = -R_{3,1}$) in $\text{Im}\chi_{zz}(\mathbf{q}, \epsilon)$ induces both a director rotation about spin 3-axis and a small spin displacement $\delta S_{j,3} \sim |\mathbf{q}|R_{3,1}$ along spin 3-axis. This spin excitation vanishes at the gapless point since the amplitude is proportional to $|\mathbf{q}|$. In the same way, fluctuations $R_{1,1}\phi_2$ and $R_{2,1}\phi_3$ in $\text{Im}\chi_{+-}(\mathbf{q}, \epsilon)$, respectively, induce spin displacements $\delta S_{j,1} \sim |\mathbf{q}|R_{1,1}$ and $\delta S_{j,2} \sim |\mathbf{q}|R_{2,1}$ together with director fluctuations. These spin excitations give finite spectral weight in dynamical spin structure factors. Near the Γ -point, the spectral weight of these director-wave (spin-wave) modes vanishes as a linear function of the momentum (or frequency),

$$\text{Im}\chi_{zz}(\mathbf{q}, \epsilon) = a_z \epsilon \delta(\epsilon - v_z |\mathbf{q}|) + \dots, \quad (71)$$

$$\text{Im}\chi_{xx}(\mathbf{q}, \epsilon) = a_x \epsilon \delta\left(\epsilon - \sqrt{v_x^2 q_x^2 + v_y^2 q_y^2}\right) + \dots, \quad (72)$$

where v_μ ($\mu = x, y, z$) denote the director-wave velocities. Mathematically, this is because the couplings $\bar{S}_{\mu;\mu}^{(1,1)}(\mathbf{q}, \epsilon)$ between spin-wave (director-wave) modes and external fields have the form $\bar{S}_{\mu;\mu}^{(1,1)}(\mathbf{q}, \epsilon) \sim \epsilon$ for small ϵ and the RPA propagators always have the form $[\bar{S}_{\mu\mu}^{(2)}(\mathbf{q}, \epsilon)]_{\alpha,\beta}^{-1} \sim \epsilon^{-1} \delta(\epsilon - \varepsilon_\mu(\mathbf{q}))$, where $\varepsilon_\mu(\mathbf{q})$ denotes the director-wave dispersion relations.

The dispersion relation of the gapless director-wave mode in $\text{Im}\chi_{zz}(\mathbf{q}, \epsilon)$ is spatially isotropic in a long-wavelength limit. The dispersion relation has a q -linear form $\varepsilon_z(\mathbf{q}) \simeq v_z |\mathbf{q}|$ near the Γ point. Contrastingly, the gapless mode in $\text{Im}\chi_{xx}(\mathbf{q}, \epsilon)$ is anisotropic even in the long-wavelength limit as $\varepsilon_x(\mathbf{q}) \simeq (v_x^2 q_x^2 + v_y^2 q_y^2)^{1/2}$, where $v_z \simeq v_x < v_y$; both the velocity and spectral weight, $a_x \epsilon = a_x (v_x^2 q_x^2 + v_y^2 q_y^2)^{1/2}$, are spatially anisotropic in the momentum space. A numerical integral of $\text{Im}\chi_{zz}$ and $\text{Im}\chi_{xx}$ with respect to ϵ for small \mathbf{q} suggests that a_z is always greater than a_x in the Z_2 planar phase.

The static magnetic susceptibilities χ_μ ($\mu = z, x$) are calculated from the dynamical spin structure factors using the relation $\chi_\mu = \lim_{\mathbf{q} \rightarrow \mathbf{0}} \int_0^\infty d\epsilon \text{Im}\chi_{\mu\mu}(\mathbf{q}, \epsilon)/\epsilon$. The collective-mode contribution to the static susceptibility comes only from the gapless modes in the $\mathbf{q} \rightarrow \mathbf{0}$ limit. The result is given by $\chi_\mu = a_\mu/\pi$. Thus, the numerical estimate concludes that χ_z is always larger than χ_x . Hence in a small magnetic field, all nematic directors are lying on the plane perpendicular to the field.

The low-energy excitations below the Stoner continuum consist also of collective modes with finite mass [see Fig. 9(b) and Fig. 10(b)]. In $\text{Im}\chi_{zz}(\mathbf{q}, \epsilon)$, there are several gapped eigenmodes near the Γ -point. Among them,

the lowest gapped eigenmode ρ_1 at the Γ -point contains in-plane antiphase oscillations of two orthogonal directors. This mode does not induce any spin excitation near Γ point, having no spectral weight in the dynamical spin structure factor $\text{Im}\chi_{zz}(\mathbf{q}, \epsilon)$. This antiphase excitation is a direct analogue of the so-called squashing modes observed in the superfluid ^3He -B phase.^{34–36} The other gapped modes come from gauge fluctuations or composite fluctuations of gauge and director (or spin) degrees of freedom. In $\text{Im}\chi_{+-}(\mathbf{q}, \epsilon)$, there are two gapped eigenmodes near Γ point, which are degenerate at Γ point. These two modes are also composite fluctuations of gauge and director degrees of freedom.

B. Near $(\pi, 0)$ -point and (π, π) -point

The vanishing spectral weight of the spin-wave modes at the Γ -point is also expected in a usual antiferromagnetic phase. In the spin-1/2 J_1 - J_2 model, a collinear antiferromagnetic ordered phase with wave vector $\mathbf{q} = (\pi, 0)$ or $(0, \pi)$ appears in the strong antiferromagnetic J_2 regime. To distinguish the Z_2 planar phase from the collinear antiferromagnetic phase, we need to look into the spin structure factor near $\mathbf{q} = (\pi, 0)$ or $(0, \pi)$. In the antiferromagnetic phase, low-energy excitations are also composed of gapless spin-wave modes at either $(\pi, 0)$ or $(0, \pi)$, whose spectral weight remains finite even at these gapless momentum points, e.g. $\text{Im}\chi_{\mu\mu}((\pi, 0) + \mathbf{q}, \epsilon) \simeq b' \delta(\epsilon - u' |\mathbf{q}|) + \dots$ for $|\mathbf{q}| \ll 1$ and $\epsilon \ll 1$. By contrast, our calculation indicates that dynamical spin structure factors in the spin nematic phase have no finite low-energy weight near $\mathbf{q} = (\pi, 0)$ and $(0, \pi)$ points, though there exist two non-magnetic linearly-gapless modes near these points in $\text{Im}\chi_{zz}(\mathbf{q}, \epsilon)$ [see Fig. 9(a)]. The zero modes at $\mathbf{q} = (\pi, 0)$ and $(0, \pi)$ are, respectively, given by \mathbf{e}_8^3 and \mathbf{e}_7^3 modes, which correspond to $\text{Re}E_{y,1}$ and $\text{Re}E_{x,2}$ fields. These modes are composite fluctuations of gauge and director degrees of freedom. Contrary to the director-wave (spin-wave) modes at the Γ point, the existence of these gapless modes at $\mathbf{q} = (\pi, 0)$ and $(0, \pi)$ are required neither by continuous spin-rotational symmetries nor by local gauge symmetries [see Appendix B], so that they could likely acquire finite mass in general situations. In the present case, the energy of a Z_2 planar state with an additional small staggered mean field $\text{Re}E_{y,1}(\mathbf{j}) = r e^{ij \cdot \mathbf{Q}_0}$ [$\mathbf{Q}_0 = (\pi, 0)$] is expanded as $E_{\text{MF}}(r)/N_\Lambda = E_{\text{MF}}(0)/N_\Lambda + cr^4$, which starts from a quartic term with a positive constant c . We hence expect that a higher-order perturbational expansion to fourth order in fluctuation fields opens a gap in the excitation energy at $\mathbf{q} = (\pi, 0)$ and $(0, \pi)$.

The energy gaps of collective modes at $\mathbf{q} = (\pi, \pi)$ are relevant to the stability of the Z_2 planar states. The lowest gapped excitations in $\text{Im}\chi_{zz}(\mathbf{q}, \epsilon)$ at $\mathbf{q} = (\pi, \pi)$

are comprised of two fluctuation fields

$$\varphi_1 = i\alpha e_1^3 + \beta e_3^3 - \gamma e_6^3 + i\delta e_9^3, \quad (73)$$

$$\varphi_2 = i\alpha e_2^3 + \beta e_4^3 - \gamma e_5^3 + i\delta e_{11}^3. \quad (74)$$

Their momentum-energy dispersions are degenerate at $\mathbf{q} = (\pi, \pi)$ [see Fig. 9(b)] due to the mirror symmetry with respect to the $(x+y)$ -axis. The lowest gapped modes in $\text{Im}\chi_{+-}(\mathbf{q}, \epsilon)$ at $\mathbf{q} = (\pi, \pi)$ are comprised of two fluctuations

$$\varphi_3 = i\epsilon e_1^2 + \zeta e_2^2, \quad \varphi_4 = i\epsilon e_1^1 + \zeta e_2^1 \quad (75)$$

[see Fig. 10(b)]. These two modes are also energetically degenerate. These four modes are composite fluctuations of gauge and director degrees of freedom. When the momentum approaches the symmetric point $\mathbf{q} = (\pi, \pi)$, the spectral weight of these four gapped modes vanishes as a quadratic function of the momentum, i.e. $\text{Im}\chi_{\mu\mu}((\pi, \pi) + \mathbf{k}, \epsilon) \simeq \alpha'' |\mathbf{k}|^2 \delta(\epsilon - m - v'' |\mathbf{k}|^2)$ for $|\mathbf{k}| \ll 1$. The vanishing of the spectral weight is a consequence of the staggered $U(1)$ spin-rotational symmetry [Eq. (22)] in the Z_2 planar state. As will be described in the next subsection, on decreasing J_2 , these four modes φ_i ($i = 1, 2, 3, 4$) become gapless at the phase boundary $J_2/J_1 = J_{c,2}$ between the adjacent $U(1)$ planar phase.

C. Transition to the $U(1)$ planar state and its instability

In the rest of this section, we briefly discuss instabilities to the Z_2 planar state, induced by energy-gap closing. In the saddle-point solution of the Z_2 planar phase⁹, when the antiferromagnetic exchange J_2 decreases, the d -wave spin-singlet pairing amplitude η is reduced to zero at the critical point $J_2/J_1 = J_{c,2} \simeq 1.0448$, while the spin-triplet pairing amplitude D and the s -wave excitonic pairing amplitude χ remain finite beyond the boundary, $J_2/J_1 < J_{c,2}$. Such a planar state in $J_2/J_1 < J_{c,2}$ is dubbed the $U(1)$ planar state, since the ansatz is invariant under the staggered $U(1)$ rotation around the 3-axis in the gauge space.

Owing to the restoration of this global $U(1)$ gauge symmetry, the gapped fluctuations φ_i ($i = 1, 2$) in the Z_2 planar state become massless gauge fluctuations at $J_2/J_1 = J_{c,2}$ [see Fig. 11(b) and Fig. 12]. To be specific, at $J_2/J_1 = J_{c,2}$, the coefficients α and γ in the fields φ_1 and φ_2 [Eqs. (73) and (74)] reduce to zero and the ratio β/δ converges to D/χ [Fig. 11(a)]. The fields have the forms

$$\varphi_1^{(c)} = D e_3^3 + i\chi e_9^3, \quad (76)$$

$$\varphi_2^{(c)} = D e_4^3 + i\chi e_{11}^3. \quad (77)$$

Such fluctuation fields are induced by generators in the

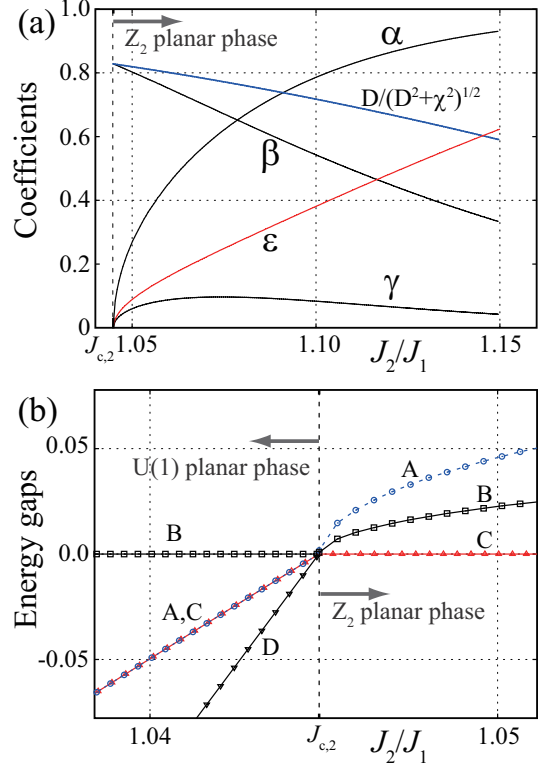


FIG. 11: (Color online) (a) Coefficients of eigenmodes φ_1 , φ_2 , and φ_3 [Eqs. (73), (74), and (75)] as a function of J_2/J_1 , where the units are taken as $\alpha^2 + \beta^2 + \gamma^2 + \delta^2 = 1$ and $\epsilon^2 + \zeta^2 = 1$. At the critical point $J_2/J_1 = J_{c,2}$ α , γ and ϵ are reduced to zero, while β , δ and ζ , respectively, converge to $D/\sqrt{D^2 + \chi^2}$, $\chi/\sqrt{D^2 + \chi^2}$ and 1. (b) Mass of eigenmodes as a function of J_2/J_1 . Negative energy gaps indicate the presence of instabilities. A: Mass of φ_3 - and φ_4 -modes at $\mathbf{q} = (\pi, \pi)$ in the Z_2 planar phase and mass of e_2^3 - and e_1^3 -modes at $\mathbf{q} = (\pi, \pi)$ in the $U(1)$ planar phase. B: Mass of φ_1 - and φ_2 -modes at $\mathbf{q} = (\pi, \pi)$. C: Mass of e_8^3 -mode at $\mathbf{q} = (\pi, 0)$ and mass of e_7^3 -mode at $\mathbf{q} = (0, \pi)$. D: Mass of e_{12}^3 -mode at $\mathbf{q} = (\pi, \pi)$.

gauge space;

$$\begin{aligned} \int_0^\beta d\tau \mathcal{L} = & S_I + \int_0^\beta d\tau \left\{ \frac{1}{2} \sum_j \text{Tr}[\Psi_j^\dagger \partial_\tau \Psi_j] \right. \\ & - \frac{J_1}{4} \sum_j \text{Tr}[\Psi_j^\dagger D \sigma_2 e^{i(-1)^{j_x+j_y} a_x^3} \sigma_3 \Psi_{j+e_x} \sigma_1^T] \\ & - \frac{J_1}{4} \sum_j \text{Tr}[\Psi_j^\dagger D \sigma_2 e^{i(-1)^{j_x+j_y} a_y^3} \sigma_3 \Psi_{j+e_y} \sigma_2^T] \\ & - \frac{J_2}{4} \sum_j \text{Tr}[\Psi_j^\dagger \chi \sigma_3 e^{i(-1)^{j_x+j_y} (a_x^3 + a_y^3)} \sigma_3 \Psi_{j+e_x+e_y}] \\ & \left. - \frac{J_2}{4} \sum_j \text{Tr}[\Psi_{j+e_x}^\dagger \chi \sigma_3 e^{-i(-1)^{j_x+j_y} (a_x^3 - a_y^3)} \sigma_3 \Psi_{j+e_y}] \right\}. \end{aligned}$$

Namely, an expansion with respect to the slowly-varying

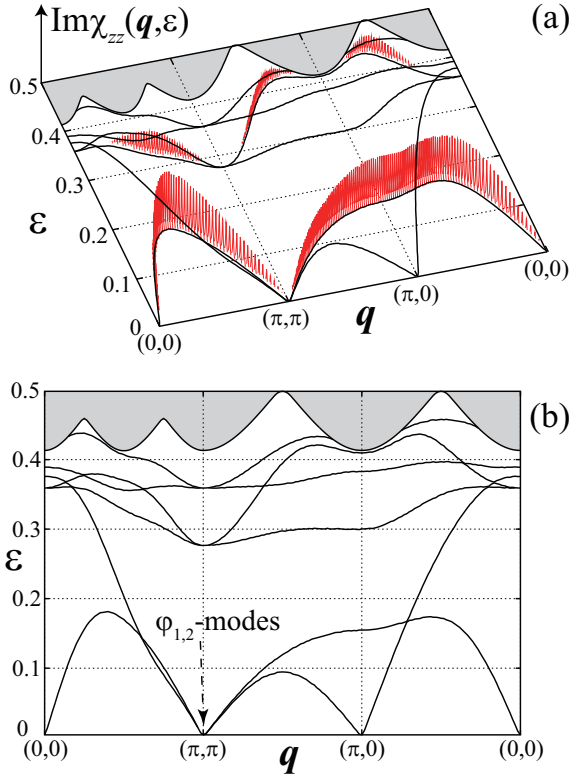


FIG. 12: (Color online) Dynamical structure factor $\text{Im}\chi_{zz}(\mathbf{q}, \epsilon)$ at the critical point $J_2/J_1 = J_{c,2} = 1.0448$ between the Z_2 planar and $U(1)$ planar phases. The grey zones denote Stoner continuum. (a) Spectral weight of the collective modes. (b) Momentum-energy dispersion relations for the collective modes, showing that the lowest excitations at the (π, π) -point become gapless.

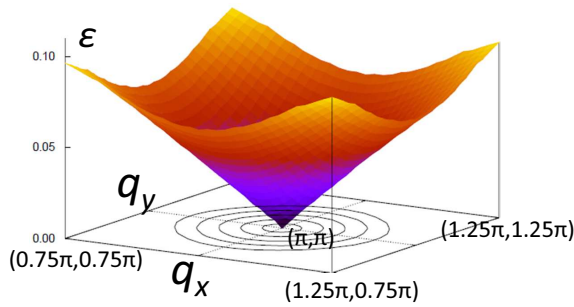


FIG. 13: (Color online) Photon-like momentum-energy dispersion in $\text{Im}\chi_{zz}(\mathbf{q}, \epsilon)$ at the (π, π) point in the $U(1)$ planar phase at $J_2/J_1 = 1.025 < J_{c,2}$.

gauge fields, $a_x^3(\mathbf{j}, \tau)$ and $a_y^3(\mathbf{j}, \tau)$, leads to

$$\int_0^\beta d\tau \mathcal{L} = \mathcal{S}_I + \frac{1}{2} \sum_{\mathbf{k}, n} \mathbf{f}_{\mathbf{k}, n}^\dagger \mathbf{g}_0^{-1}(\mathbf{k}, i\omega_n) \mathbf{f}_{\mathbf{k}, n} + \frac{1}{\sqrt{\beta N_\Lambda}} \times \sum_{\alpha=1}^{35} \sum_{\mathbf{q}, m} \sum_{\mathbf{k}, n} \mathbf{f}_{\mathbf{k}, n}^\dagger \mathbf{v}_\alpha(\mathbf{k}, \mathbf{k} - (\pi, \pi) - \mathbf{q}) \mathbf{f}_{\mathbf{k} - (\pi, \pi) - \mathbf{q}, n-m} \times \left\{ a_x^3(\mathbf{q}, i\omega_m) \varphi_{1, \alpha}^{(c)} + a_y^3(\mathbf{q}, i\omega_m) \varphi_{2, \alpha}^{(c)} \right\},$$

where $\varphi_{1, \alpha}^{(c)}$ and $\varphi_{2, \alpha}^{(c)}$ are exactly given by Eqs. (76) and (77). An integration over the fermion field and subsequent expansion of the action in terms of a_x^3 and a_y^3 leads to a quadratic form of the effective action, $\sum_{\mathbf{q}, i\omega_n, \alpha, \beta} M_{\alpha\beta}(\mathbf{q}, i\omega_n) a_\alpha(\mathbf{q}, i\omega_n) a_\beta(-\mathbf{q}, -i\omega_n)$. Now that the $U(1)$ planar state is invariant under the staggered $U(1)$ rotation around the 3-axis in the gauge space, the effective action thus obtained is transformed into $\sum M_{\alpha\beta}(\mathbf{q}, i\omega_n) (a_\alpha + \partial_\alpha \theta)(\mathbf{q}, i\omega_n) (a_\beta + \partial_\beta \theta)(-\mathbf{q}, -i\omega_n)$ under a $U(1)$ local gauge transformation; $\Psi_j^\dagger \rightarrow \Psi_j^\dagger e^{i(-1)^{j_x+j_y} \theta(\mathbf{r}) \sigma_3}$ with slowly varying function $\theta(\mathbf{r})$. On the one end, any physical quantities including the action should have been invariant under any local gauge transformation, which enforces $M_{\alpha\beta}(\mathbf{q} = 0, i\omega_n = 0)$ to be zero precisely. More accurately, it is required that a_x^3 and a_y^3 in combination with the staggered component of the temporal gauge field, i.e. $a_0^3 \equiv (-1)^{j_x+j_y} a_{\mathbf{j}, \tau}^3$, must take a gauge invariant quadratic form as their effective action, which turns out to be the Maxwell form⁹

$$F_{\text{gauge}} = \int_0^\beta d\tau \int d^2r \left(u \mathbf{E}^2 + \frac{K}{2} B^2 \right). \quad (78)$$

The ‘emergent’ electromagnetic fields are defined as $E_\alpha \equiv \partial_\tau a_\alpha^3 - \partial_\alpha a_0^3$, and $B \equiv \partial_x a_y^3 - \partial_y a_x^3$.

In the 2 + 1 dimensional space, this Maxwell form does not suppress the fluctuations of these gauge fields efficiently, so that the $U(1)$ planar state is generally unstable against these fluctuations. That is, the space-time instanton which is allowed by the corresponding compact QED action, $\int_0^\beta \int d^2r \{ u \mathbf{E}^2 - K \cos(\epsilon_{\alpha\beta} \partial_\alpha a_\beta^3) \}$, proliferate in the 2 + 1 dimensional space, only to introduce strong confining potentials between two neutral ‘free’ fermions (spinon).³⁷ In the context of spin-singlet quantum spin liquids, it is known that resulting confining phases are accompanied by the reduction of the space group symmetry of original mean-field states.³⁸

In the present situation, this symmetry reduction is driven by the condensation of φ_3 -, φ_4 -, and \mathbf{e}_{12}^3 -modes at $\mathbf{q} = (\pi, \pi)$, \mathbf{e}_3^3 -mode at $\mathbf{q} = (\pi, 0)$, and \mathbf{e}_7^3 -mode at $\mathbf{q} = (0, \pi)$, where \mathbf{e}_{12}^3 originates from the unphysical zero modes mentioned in the previous section. As shown in Fig. 11(b), the mass of these modes are all negative in the $U(1)$ phase, $J_2/J_1 < J_{c,2}$, where φ_3 - and φ_4 -modes are transformed into \mathbf{e}_2^3 and \mathbf{e}_2^1 respectively [see Fig. 11(a)]. We thus expect that the $U(1)$ phase is generally accompanied by condensations of $\text{Im}D_{x,3}$, $\text{Im}D_{y,3}$,

$\text{Im}\eta_{x+y}-\text{Im}\eta_{x-y}$ with $\mathbf{q} = (\pi, \pi)$, $\text{Re}E_{y,1}$ with $\mathbf{q} = (\pi, 0)$, and $\text{Re}E_{x,2}$ with $\mathbf{q} = (0, \pi)$. Such condensations break the time-reversal symmetry \mathcal{T} , the π spin-rotation symmetry around the z -axis $\mathcal{R}_{\pi,z}^{\text{spin}}$ and the translational symmetries T_μ ($\mu = x, y$). These symmetry breakings would possibly endow the $U(1)$ phase with ferrimagnetic moments. Having such magnetic orderings in the background, a pair of spinon and anti-spinon introduced in the $U(1)$ planar phase generally pay those energy cost which are proportional to the spatial distance between these two.^{3,4,39} Because of this strong confining potential, the pair is spatially confined to each other in the $U(1)$ planar phase.

We note that this $U(1)$ planar state does not survive as a stable ground state if the mean-field solutions are projected to the real spin space²⁶. It is hence expected that the transition from the Z_2 planar state to the $U(1)$ planar state appears only in the large- N spin model.

D. Transition to the π -flux states

When the antiferromagnetic exchange J_2 increases in the Z_2 planar phase, the spin-triplet pairing field D decreases and vanishes at $J_2/J_1 = J_{c,1} \simeq 1.325$, while the other two remains almost constant. In $J_2/J_1 \geq J_{c,1}$, the saddle-point solution is a π -flux state having $D = 0$ and $\chi = \eta \neq 0$, where the Stoner excitations become gapless at five (inequivalent) symmetric momentum points $(0, 0)$, $(\pi/2, \pi/2)$, (π, π) , $(\pi, 0)$ and $(0, \pi)$. Correspondingly, all the collective excitations and their spectral weight in the spin structure factor merge into the lower edge of the Stoner continuum, when J_2/J_1 gets closer to the critical value $J_{c,1}$ from below. We note that in the usual $N = 1$ $S = 1/2$ spin model this π -flux phase becomes a collinear antiferromagnetic phase²⁶. It is hence expected that the transition from the Z_2 planar phase to the π -flux phase appears only in the large- N model.

V. NMR RELAXATION TIME

In the previous section, we have observed that the spectral weight of gapless spin-wave (director-wave) modes vanishes as a linear function of the momentum near the Γ point. These modes are the only magnetic low-lying excitations in the Z_2 planar state. This behavior is also observed theoretically in other kinds of spin nematic phases^{31,40} and can be regarded as a common property of quantum spin nematics in $d \geq 2$.²³ In this section, we will calculate the longitudinal relaxation time T_1 of the nuclear magnetic resonance (NMR) in the spin nematic phase, which also captures a low-energy property of the dynamical spin structure factor through the relation

$$\frac{1}{T_1} = \frac{2\gamma_n^2 T}{\hbar^2 \gamma_e^2} \lim_{\omega \rightarrow 0} \sum_{\mu=1}^3 \sum_{\mathbf{q}} A_\mu \frac{\text{Im}\chi_{\mu\mu}(\mathbf{q}, \omega)}{\omega}. \quad (79)$$

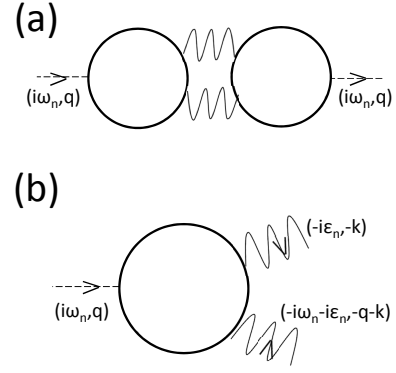


FIG. 14: (a) Raman scattering process. (b) Each vertex part consists of two internal lines (wavy lines; gapless director-wave modes) and one external line (dashed line; magnetic field).

Here, γ_e and γ_n stand for the gyromagnetic ratio of electron spin and nuclear spin, respectively, and A_μ ($\mu = x, y, z$) denote the form factors, which depend on the geometry of couplings between nuclear spins and electron spins.^{41,43} We argue that the low-temperature behavior of the NMR relaxation rate $1/T_1$ also exhibits a characteristic temperature dependence.

When the temperature is sufficiently low, nuclear spins relaxations are mainly attributed to the scattering processes involved with the gapless spin-wave modes. There are two types of relevant scattering processes:⁴¹ one is (i) a direct process, in which a nuclear spin is flipped by either one-magnon emission or one-magnon absorption. As in usual magnetic Mott insulators, the direct process in spin nematic phases is forbidden in usual experimental situations, because all magnetic compounds inevitably contain tiny spin-anisotropy fields, such as Dzyaloshinsky-Moriya exchange field and dipolar field, which opens a gap relatively larger than the nuclear Larmor frequency. In such cases, the scattering process is dominated by (ii) the so-called Raman process, where a nuclear spin flipping is accompanied by the simultaneous occurrence of one-magnon emission and one-magnon absorption.

In the framework of the $1/N$ expansion, this Raman process can be captured by a 2-loop diagram of order $1/N^2$ which has simultaneous two fluctuation-field propagators between the two loops, as depicted in Fig. 14(a). Here, two fluctuation-field propagators (wavy lines) correspond to magnon (director-wave) emission and absorption. In the following, we will argue that this Raman contribution results in a characteristic low-temperature dependence of the NMR relaxation rate,

$$\frac{1}{T_1} = aT^{2d-1} + \dots \quad (80)$$

[see Eq. (84)], where d denotes the (effective) spatial dimension.⁴²

The Raman process shown in Fig. 14(a) consists of two vertex parts $\tilde{\mathcal{S}}^{(1,2)}$, each of which has one external

	h_x	h_y	h_z	ϕ_1	ϕ_2	ϕ_3
\mathcal{T}	$-h_x$	$-h_y$	$-h_z$	ϕ_1	ϕ_2	ϕ_3
σ_x	h_x	h_y	h_z	ϕ_1	ϕ_2	ϕ_3
σ_y	h_x	h_y	h_z	ϕ_1	ϕ_2	ϕ_3
$R_{\frac{\pi}{2},z}$	h_y	$-h_x$	h_z	ϕ_1	ϕ_3	ϕ_2
$R_{\pi,z}^{\text{spin}}$	$-h_x$	$-h_y$	h_z	ϕ_1	$-\phi_2$	$-\phi_3$

TABLE I: Transformation properties of gapless director-wave modes under time-reversal \mathcal{T} , mirror operations σ_μ with respect to the μ -axis, and rotations in spin and lattice space. $R_{\frac{\pi}{2},z} \equiv R_{\frac{\pi}{2},z}^{\text{spin}} R_{\frac{\pi}{2},z}^{\text{lat}}$, where $R_{\theta,z}^{\text{spin/lat}}$ denotes the spin(lattice)-rotation by θ around the z -axis. Note that \mathcal{T} , σ_x , σ_y , $R_{\frac{\pi}{2},z}$, and $R_{\pi,z}^{\text{spin}}$ are, respectively, accompanied by proper gauge transformations, $\Psi_j^\dagger \rightarrow \Psi_j^\dagger(-1)^{j_x+j_y}$, $\Psi_j^\dagger \rightarrow \Psi_j^\dagger \sigma_1(-1)^{j_x}$, $\Psi_j^\dagger \rightarrow \Psi_j^\dagger \sigma_1(-1)^{j_y}$, $\Psi_j^\dagger \rightarrow \Psi_j^\dagger \sigma_1(-1)^{j_y}$, and $\Psi_j^\dagger \rightarrow \Psi_j^\dagger(-1)^{j_x+j_y}$.

(dashed) line representing magnetic field and two internal (wavy) lines representing the fluctuating modes. Among the fluctuating modes, the gapless director-wave modes (ϕ_1 , ϕ_2 , and ϕ_3) with low frequencies only contribute to the relaxation rate at sufficiently low temperature. We first determine a form of the vertex part $\bar{\mathcal{S}}^{(1,2)}$ associated with these gapless modes by using a symmetry argument. Under the time-reversal transformation combined with a proper gauge transformation $\Psi_j^\dagger \rightarrow \Psi_j^\dagger(-1)^{j_x+j_y}$ and $\Psi_j \rightarrow (-1)^{j_x+j_y} \Psi_j$, none of the director-wave modes changes its sign, while external magnetic field changes the sign. Since the interaction $\mathcal{S}^{(1,2)} h_\mu \phi_j \phi_m$ respects the time-reversal symmetry, the vertex part $\bar{\mathcal{S}}^{(1,2)}$ is an odd function of frequency. Expanding the vertex part $\bar{\mathcal{S}}^{(1,2)}$ of Fig. 14(b) with frequencies $i\omega_n$ and $i\epsilon_n$, we obtain a linear function of

$$i\omega_n h_\mu(i\omega_n, \mathbf{q}) \phi_j(i\epsilon_n, \mathbf{k}) \phi_m(-i\epsilon_n - i\omega_n, -\mathbf{q} - \mathbf{k}) \quad (81)$$

and

$$i\epsilon_n h_\mu(i\omega_n, \mathbf{q}) \phi_j(i\epsilon_n, \mathbf{k}) \phi_m(-i\epsilon_n - i\omega_n, -\mathbf{q} - \mathbf{k}), \quad (82)$$

where $\mu = x, y, z$ and $j, m = 1, 2, 3$, in the leading term. Since third- and higher-order time-derivative terms lead to subleading contributions in the relaxation rate, we will consider only the first-order time-derivative terms. Transformation properties of the gapless director-wave modes under other symmetry operations (see Table. I) further restrict allowed combinations of μ , j and m in Eqs. (81) and (82) to the following sets

$$\begin{aligned} & i\omega_n h_z \phi_1 \phi_1, \quad i\omega_n h_z \phi_2 \phi_2, \quad i\omega_n h_z \phi_3 \phi_3, \quad i\omega_n h_z \phi_2 \phi_3, \\ & i\epsilon_n (h_x \phi_1 \phi_2 - h_y \phi_1 \phi_3), \quad (i\epsilon_n + i\omega_n) (h_x \phi_1 \phi_2 - h_y \phi_1 \phi_3), \\ & i\epsilon_n (h_x \phi_1 \phi_3 - h_y \phi_1 \phi_2), \quad (i\epsilon_n + i\omega_n) (h_x \phi_1 \phi_3 - h_y \phi_1 \phi_2), \end{aligned}$$

where we have omitted momentum and frequency arguments in h_μ and ϕ_i .

Taking the contractions between the two internal lines that connects two vertex parts in Fig. 14(a), we can see

that this Raman contribution always takes the following form

$$\begin{aligned} \chi_{\mu\mu}^{\text{ram}}(\mathbf{q}, i\omega_n) = & \frac{1}{\beta} \sum_{\mathbf{k}} \sum_{\epsilon_n} \frac{\alpha_\mu \omega_n^2 + \beta_\mu (\omega_n + \epsilon_n) \epsilon_n + \gamma_\mu \omega_n \epsilon_n}{[(\omega_n + \epsilon_n)^2 + \varepsilon_1^2] (\epsilon_n^2 + \varepsilon_2^2)}, \end{aligned}$$

where $\varepsilon_1 \equiv \varepsilon_{-\mathbf{k}-\mathbf{q}}$ and $\varepsilon_2 \equiv \varepsilon_{\mathbf{k}}$ correspond to the energies of the gapless director-wave modes. For simplicity, we assumed that the momentum-energy dispersions of these three linearly-gapless modes are all the same, while their difference does not change the conclusion on the leading temperature dependence, i.e., Eq. (80). The coefficients α_μ , β_μ , and γ_μ ($\mu = x, y, z$) are determined by specific microscopic evaluations of the vertex part. As far as the leading-order contribution is concerned, we can treat these coefficients as constants independent of momentum and frequency.

With the analytic continuation, $i\omega_n \rightarrow \omega + i\delta$, the Raman contribution to the imaginary part of the dynamical susceptibilities can be calculated as

$$\begin{aligned} \text{Im} \chi_{\mu\mu}^{\text{ram}}(\mathbf{q}, \omega) = & \text{Im} \chi_{\mu\mu}^{\text{ram}}(\mathbf{q}, i\omega_n = \omega + i\delta) \\ = & \sum_{\mathbf{k}} \left(\frac{\alpha_\mu \pi \omega^2}{4\varepsilon_1 \varepsilon_2} + \frac{\beta_\mu \pi}{4} + \frac{\gamma_\mu \pi \omega}{4\varepsilon_1} \right) [n^{\text{B}}(\varepsilon_1) - n^{\text{B}}(\varepsilon_2)] \\ & \times \delta(\omega - \varepsilon_1 + \varepsilon_2) \\ - & \sum_{\mathbf{k}} \left(\frac{\alpha_\mu \pi \omega^2}{4\varepsilon_1 \varepsilon_2} + \frac{\beta_\mu \pi}{4} - \frac{\gamma_\mu \pi \omega}{4\varepsilon_1} \right) [n^{\text{B}}(\varepsilon_1) - n^{\text{B}}(\varepsilon_2)] \\ & \times \delta(\omega + \varepsilon_1 - \varepsilon_2), \end{aligned}$$

where $n^{\text{B}}(\varepsilon)$ denotes the Bose distribution function, $n^{\text{B}}(\varepsilon) = (e^{\beta\varepsilon} - 1)^{-1}$. Since ω will be replaced by zero (tiny nuclear Raman frequency), we have dropped those terms which are proportional to either $\delta(\omega - \varepsilon_1 - \varepsilon_2)$ or $\delta(\omega + \varepsilon_1 + \varepsilon_2)$, while keeping those terms which are proportional to either $\delta(\omega - \varepsilon_1 + \varepsilon_2)$ or $\delta(\omega + \varepsilon_1 - \varepsilon_2)$. In terms of density of state for the gapless mode defined as $N(\omega) = \sum_{\mathbf{k}} \delta(\omega - \varepsilon_{\mathbf{k}})$, we obtain an expression for the NMR relaxation rate as

$$\begin{aligned} \frac{1}{T_1} = & \lim_{\omega \rightarrow 0} \frac{\pi \gamma_n^2 T}{\hbar^2 \gamma_e^2 \omega} \\ & \times \int_0^\Lambda d\Omega \left\{ [n^{\text{B}}(\omega + \Omega) - n^{\text{B}}(\Omega)] N(\Omega) N(\Omega + \omega) \right. \\ & \times \left(\frac{\mathbf{A} \cdot \boldsymbol{\alpha} \omega^2}{(\omega + \Omega)\Omega} + \mathbf{A} \cdot \boldsymbol{\beta} + \frac{\mathbf{A} \cdot \boldsymbol{\gamma} \omega}{(\omega + \Omega)} \right) \\ & - [n^{\text{B}}(-\omega + \Omega) - n^{\text{B}}(\Omega)] N(\Omega) N(\Omega - \omega) \\ & \times \left. \left(\frac{\mathbf{A} \cdot \boldsymbol{\alpha} \omega^2}{(-\omega + \Omega)\Omega} + \mathbf{A} \cdot \boldsymbol{\beta} - \frac{\mathbf{A} \cdot \boldsymbol{\gamma} \omega}{(-\omega + \Omega)} \right) \right\}, \quad (83) \end{aligned}$$

where $\mathbf{A} = (A_x, A_y, A_z)$, $\boldsymbol{\alpha} = (\alpha_x, \alpha_y, \alpha_z)$, $\boldsymbol{\beta} = (\beta_x, \beta_y, \beta_z)$, and $\boldsymbol{\gamma} = (\gamma_x, \gamma_y, \gamma_z)$. We assume that the form factors A_μ ($\mu = x, y, z$) have neither temperature

dependence nor momentum dependence. Since $N(\Omega) \propto \Omega^{d-1}$ in d dimensions, we can evaluate the temperature dependence of the relaxation rate in the low-temperature limit as

$$\frac{1}{T_1} = \frac{2\pi \gamma_n^2 T^{2d-1}}{\hbar^2 \gamma_e^2} \int_0^\infty dX f(X), \quad (84)$$

where $f(X)$ is free from the temperature and given by

$$f(X) = \frac{d}{dx} \left\{ [\bar{n}^B(x+X) - \bar{n}^B(X)] N(X)N(X+x) \times \left(\frac{\mathbf{A} \cdot \boldsymbol{\alpha} x^2}{(x+X)X} + \mathbf{A} \cdot \boldsymbol{\beta} + \frac{\mathbf{A} \cdot \boldsymbol{\gamma} x}{(x+X)} \right) \right\} \Big|_{x=0}$$

with

$$\bar{n}^B(x) = \frac{1}{e^x - 1}.$$

VI. SUMMARY

We have studied dynamical properties of a spin nematic state called Z_2 planar state in a generalized N -flavor spin-1/2 J_1 - J_2 model on the square lattice. In the large- N limit, the Z_2 planar state is the ground state in a finite parameter range⁹ in which ferromagnetic coupling J_1 competes strongly with the antiferromagnetic coupling J_2 . The Z_2 planar state has the completely same magnetic properties,²⁶ including an antiferro-quadrupolar order, as the d -wave spin nematic state proposed in the spin-1/2 J_1 - J_2 model ($N=1$) on the square lattice. Using the standard $1/N$ expansion, we have calculated the dynamical spin-structure factors up to order of $1/N$ in this quantum spin nematic state for large N .

The obtained dynamical spin structure factors have two characters; they have both a spin-liquid like character and a symmetry-broken phase character. The former feature is represented by the so-called Stoner continuum of individual excitations of gapped neutral fermions (spinons). Due to the existence of an antiferro-quadrupolar order, the dynamical spin structure factors also acquire coherent peaks below the continuum, which signifies the existence of gapless director-wave (spin-wave) collective modes. These director-wave modes have linear dispersions with respect to the momentum in the long-wavelength limit. These director fluctuations are accompanied with weak spin excitations and hence they have a finite spectral weight in the dynamical spin structure factors, which is proportional to the momentum, e.g. $\text{Im}\chi_{zz}(\mathbf{q}, \epsilon) \simeq a_z v_z |\mathbf{q}| \delta(\epsilon - v_z |\mathbf{q}|)$. A careful analysis revealed that these q -linear modes are the only magnetic

low-energy excitations in this spin nematic state. Accordingly, temperature dependence of (magnetic contributions to) the specific heat in the present spin nematic phase can be evaluated as a quadratic function of temperature, $C_v \sim T^2$, in the low- T regime, while that of the NMR relaxation rate is evaluated as $T_1^{-1} \sim T^3$. The latter unusual behavior of the NMR relaxation rate was also discussed in an antiferro-quadrupolar phase in a spin-1 bilinear-biquadratic model.³¹

The lowest gapped excitations around $\mathbf{q} = (\pi, \pi)$ are identified as a certain kind of Higgs bosons, whose finite mass quantifies the stability of the present Z_2 planar phase against the ‘confinement effect’. Though these massive modes are gauge-like excitations, they have finite spectral weight in the dynamical *spin* structure factor, once the momentum is deviated from $\mathbf{q} = (\pi, \pi)$. Thus the mass can be experimentally measured with inelastic neutron scattering experiments. When these Higgs bosons lose their mass, which is the case near the ferromagnetic phase boundary for large N ,⁹ a ‘linear’ confining potential should be introduced between two neutral fermions and the Z_2 planar phase is transformed into another phase having *no* gapped free spinon. We also found that, at this transition point, a couple of other gapped bosonic modes at high symmetric momentum points simultaneously exhibit instabilities, which break the time-reversal symmetry, a spin- π -rotational symmetry, and the translational symmetries of the square lattice.

Acknowledgments

We acknowledge Masahiro Sato, Kazutaka Takahashi, Akira Furusaki, Andrey Chubukov, Leon Balents, Kimi-toshi Kono, Nic Shannon, and Andrew Smerald for helpful discussions. We also thank to Sebastien Burdin for his insightful comment on the nature of the $U(1)$ planar phase. RS was partially supported by the Institute of Physical and Chemical Research (RIKEN). This work was supported by Grants-in-Aid for Scientific Research from MEXT, Japan (No. 22014016 and No. 23540397).

Appendix A: Explicit expressions for Eqs. (64) and (66)

The RPA propagators $\bar{\mathcal{S}}_{jj}^{(0,2)}(q, i\epsilon_n)$ ($j = 1, 2, 3$), defined in Eq. (64), are calculated as follows:

$$\overline{\mathcal{S}}_{33}^{(0,2)} \equiv \begin{matrix} \begin{matrix} e_3^3 \\ e_{3,3}^3 \\ e_{3,3,3}^3 \\ e_{3,3,3,3}^3 \\ e_{3,3,3,3,3}^3 \\ e_{3,3,3,3,3,3}^3 \\ e_{3,3,3,3,3,3,3}^3 \\ e_{3,3,3,3,3,3,3,3}^3 \\ e_{3,3,3,3,3,3,3,3,3}^3 \\ e_{3,3,3,3,3,3,3,3,3,3}^3 \\ e_{3,3,3,3,3,3,3,3,3,3,3}^3 \\ e_{3,3,3,3,3,3,3,3,3,3,3,3}^3 \end{matrix} & \begin{pmatrix} e_1^3 & e_2^3 & e_3^3 & e_4^3 & e_5^3 & e_6^3 & e_7^3 & e_8^3 & e_9^3 & e_{10}^3 & e_{11}^3 & e_{12}^3 \\ \alpha_1 & \beta_{1,2} & \beta_{1,3} & & \beta_{1,5} & & \beta_{1,7} & & \beta_{1,9} & & \beta_{1,11} & \\ \beta_{1,2} & \alpha_2 & & \beta_{2,4} & & \beta_{2,6} & & \beta_{2,8} & \beta_{2,9} & & \beta_{2,11} & \\ -\beta_{1,3} & & \alpha_3 & \beta_{3,4} & \beta_{3,5} & & \beta_{3,7} & & \beta_{3,9} & \beta_{3,10} & \beta_{3,11} & \beta_{3,12} \\ & -\beta_{2,4} & \beta_{3,4} & \alpha_4 & & \beta_{4,6} & & \beta_{4,8} & \beta_{4,9} & \beta_{4,10} & \beta_{4,11} & \beta_{4,12} \\ -\beta_{1,5} & & \beta_{3,5} & & \alpha_5 & \beta_{5,6} & \beta_{5,7} & & \beta_{5,9} & \beta_{5,10} & \beta_{5,11} & \beta_{5,12} \\ & -\beta_{2,6} & & \beta_{4,6} & \beta_{5,6} & \alpha_6 & & \beta_{6,8} & \beta_{6,9} & \beta_{6,10} & \beta_{6,11} & \beta_{6,12} \\ -\beta_{1,7} & & \beta_{3,7} & & \beta_{5,7} & & \alpha_7 & \beta_{7,8} & & \beta_{7,10} & & \beta_{7,12} \\ & -\beta_{2,8} & & \beta_{4,8} & & \beta_{6,8} & \beta_{7,8} & \alpha_8 & & \beta_{8,10} & & \beta_{8,12} \\ \beta_{1,9} & \beta_{2,9} & -\beta_{3,9} & -\beta_{4,9} & -\beta_{5,9} & -\beta_{6,9} & & & \alpha_9 & \beta_{9,10} & \beta_{9,11} & \beta_{9,12} \\ & & \beta_{3,10} & \beta_{4,10} & \beta_{5,10} & \beta_{6,10} & \beta_{7,10} & \beta_{8,10} & -\beta_{9,10} & \alpha_{10} & \beta_{10,11} & \beta_{10,12} \\ \beta_{1,11} & \beta_{2,11} & -\beta_{3,11} & -\beta_{4,11} & -\beta_{5,11} & -\beta_{6,11} & & & \beta_{9,11} & -\beta_{10,11} & \alpha_{11} & \beta_{11,12} \\ & & \beta_{3,12} & \beta_{4,12} & \beta_{5,12} & \beta_{6,12} & \beta_{7,12} & \beta_{8,12} & -\beta_{9,12} & \beta_{10,12} & -\beta_{11,12} & \alpha_{12} \end{pmatrix} \end{pmatrix} \quad (A1)$$

$$\overline{\mathcal{S}}_{11}^{(0,2)} \equiv \begin{matrix} e_1^1 & e_2^1 & e_3^1 & e_4^1 \\ e_1^1 & \begin{pmatrix} \alpha'_1 & \beta'_{1,2} & \beta'_{1,3} & \beta'_{1,4} \\ -\beta'_{1,2} & \alpha'_2 & \beta'_{2,3} & \beta'_{2,4} \\ -\beta'_{1,3} & \beta'_{2,3} & \alpha'_3 & \beta'_{3,4} \\ -\beta'_{1,4} & \beta'_{2,4} & \beta'_{3,4} & \alpha'_4 \end{pmatrix} \\ e_3^1 & \\ e_4^1 & \end{matrix} \quad (A2)$$

and

$$\overline{\mathcal{S}}_{22}^{(0,2)} \equiv \begin{matrix} e_1^2 & e_2^2 & e_3^2 & e_4^2 \\ e_1^2 & \begin{pmatrix} \alpha''_1 & \beta''_{1,2} & \beta''_{1,3} & \beta''_{1,4} \\ -\beta''_{1,2} & \alpha''_2 & \beta''_{2,3} & \beta''_{2,4} \\ -\beta''_{1,3} & \beta''_{2,3} & \alpha''_3 & \beta''_{3,4} \\ -\beta''_{1,4} & \beta''_{2,4} & \beta''_{3,4} & \alpha''_4 \end{pmatrix} \\ e_3^2 & \\ e_4^2 & \end{matrix} \quad (A3)$$

Respective matrix elements are calculated as follows:

$$\alpha_1 = \frac{1}{N_\Lambda} \sum_{\mathbf{k}} s_x^2 \{ h_{\mathbf{k}} - (\xi_+ \xi_- - 2a_{5,+} a_{5,-}) f_{\mathbf{k}} \} - \frac{1}{N_\Lambda} \sum_{\mathbf{k}} s_x^2 \{ h_{\mathbf{k}}^0 - \xi^2 f_{\mathbf{k}}^0 \}, \quad (A4)$$

$$\alpha_2 = \frac{1}{N_\Lambda} \sum_{\mathbf{k}} s_y^2 \{ h_{\mathbf{k}} - (\xi_+ \xi_- - 2a_{3,+} a_{3,-}) f_{\mathbf{k}} \} - \frac{1}{N_\Lambda} \sum_{\mathbf{k}} s_y^2 \{ h_{\mathbf{k}}^0 - \xi^2 f_{\mathbf{k}}^0 \}, \quad (A5)$$

$$\alpha_3 = \frac{1}{N_\Lambda} \sum_{\mathbf{k}} s_y^2 \{ h_{\mathbf{k}} - (\xi_+ \xi_- - 2a_{2,+} a_{2,-} - 2a_{3,+} a_{3,-}) f_{\mathbf{k}} \} - \frac{1}{N_\Lambda} \sum_{\mathbf{k}} s_y^2 \{ h_{\mathbf{k}}^0 - \xi^2 f_{\mathbf{k}}^0 \}, \quad (A6)$$

$$\alpha_4 = \frac{1}{N_\Lambda} \sum_{\mathbf{k}} s_x^2 \{ h_{\mathbf{k}} - (\xi_+ \xi_- - 2a_{2,+} a_{2,-} - 2a_{5,+} a_{5,-}) f_{\mathbf{k}} \} - \frac{1}{N_\Lambda} \sum_{\mathbf{k}} s_x^2 \{ h_{\mathbf{k}}^0 - \xi^2 f_{\mathbf{k}}^0 \}, \quad (A7)$$

$$\alpha_5 = \frac{1}{N_\Lambda} \sum_{\mathbf{k}} s_y^2 \{ h_{\mathbf{k}} - (\xi_+ \xi_- - 2a_{3,+} a_{3,-} - 2a_{4,+} a_{4,-}) f_{\mathbf{k}} \} - \frac{1}{N_\Lambda} \sum_{\mathbf{k}} s_y^2 \{ h_{\mathbf{k}}^0 - \xi^2 f_{\mathbf{k}}^0 \}, \quad (A8)$$

$$\alpha_6 = \frac{1}{N_\Lambda} \sum_{\mathbf{k}} s_x^2 \{ h_{\mathbf{k}} - (\xi_+ \xi_- - 2a_{4,+} a_{4,-} - 2a_{5,+} a_{5,-}) f_{\mathbf{k}} \} - \frac{1}{N_\Lambda} \sum_{\mathbf{k}} s_x^2 \{ h_{\mathbf{k}}^0 - \xi^2 f_{\mathbf{k}}^0 \}, \quad (A9)$$

$$\alpha_7 = \frac{1}{N_\Lambda} \sum_{\mathbf{k}} c_x^2 \{ h_{\mathbf{k}} - (\xi_+ \xi_- - 2a_{2,+} a_{2,-} - 2a_{4,+} a_{4,-} - 2a_{5,+} a_{5,-}) f_{\mathbf{k}} \} - \frac{1}{N_\Lambda} \sum_{\mathbf{k}} s_x^2 \{ h_{\mathbf{k}}^0 - \xi^2 f_{\mathbf{k}}^0 \}, \quad (A10)$$

$$\alpha_8 = \frac{1}{N_\Lambda} \sum_{\mathbf{k}} c_y^2 \{ h_{\mathbf{k}} - (\xi_+ \xi_- - 2a_{2,+} a_{2,-} - 2a_{3,+} a_{3,-} - 2a_{4,+} a_{4,-}) f_{\mathbf{k}} \} - \frac{1}{N_\Lambda} \sum_{\mathbf{k}} s_y^2 \{ h_{\mathbf{k}}^0 - \xi^2 f_{\mathbf{k}}^0 \}, \quad (A11)$$

where $\frac{J^2}{4}$ were omitted from the overall factors in the right hand sides.

$$\alpha_9 = \frac{2}{N_\Lambda} \sum_{\mathbf{k}} c_y^2 \{ s_x^2 (h_{\mathbf{k}} + \xi_+ \xi_- f_{\mathbf{k}}) - c_x^2 (h_{\mathbf{k}}^0 - \xi^2 f_{\mathbf{k}}^0) \}, \quad (A12)$$

$$\alpha_{11} = \frac{2}{N_\Lambda} \sum_{\mathbf{k}} c_x^2 \{ s_y^2 (h_{\mathbf{k}} + \xi_+ \xi_- f_{\mathbf{k}}) - c_y^2 (h_{\mathbf{k}}^0 - \xi^2 f_{\mathbf{k}}^0) \}, \quad (A13)$$

$$\alpha_{10} = \frac{1}{N_\Lambda} \sum_{\mathbf{k}} 2c_x^2 c_y^2 \{h_{\mathbf{k}} - (\xi_+ \xi_- - 2a_{3,+} a_{3,-} - 2a_{5,+} a_{5,-}) f_{\mathbf{k}}\} - \frac{1}{N_\Lambda} \sum_{\mathbf{k}} 2c_x^2 c_y^2 \{h_{\mathbf{k}}^0 - \xi^2 f_{\mathbf{k}}^0\}, \quad (\text{A14})$$

$$\alpha_{12} = \frac{1}{N_\Lambda} \sum_{\mathbf{k}} 2s_x^2 s_y^2 \{h_{\mathbf{k}} - (\xi_+ \xi_- - 2a_{3,+} a_{3,-} - 2a_{5,+} a_{5,-}) f_{\mathbf{k}}\} - \frac{1}{N_\Lambda} \sum_{\mathbf{k}} 2s_x^2 s_y^2 \{h_{\mathbf{k}}^0 - \xi^2 f_{\mathbf{k}}^0\}, \quad (\text{A15})$$

where $\frac{J_2^2}{4}$ were omitted from the overall factors in the right hand sides.

$$\alpha'_1 = \frac{1}{N_\Lambda} \sum_{\mathbf{k}} s_y^2 \{h_{\mathbf{k}} - \xi_+ \xi_- f_{\mathbf{k}} - h_{\mathbf{k}}^0 + \xi^2 f_{\mathbf{k}}^0\}, \quad (\text{A16})$$

$$\alpha'_2 = \frac{1}{N_\Lambda} \sum_{\mathbf{k}} s_x^2 \{h_{\mathbf{k}} - (\xi_+ \xi_- - 2a_{2,+} a_{2,-} - 2a_{3,+} a_{3,-} - 2a_{5,+} a_{5,-}) f_{\mathbf{k}}\} - \frac{1}{N_\Lambda} \sum_{\mathbf{k}} s_x^2 \{h_{\mathbf{k}}^0 - \xi^2 f_{\mathbf{k}}^0\}, \quad (\text{A17})$$

$$\alpha'_3 = \frac{1}{N_\Lambda} \sum_{\mathbf{k}} s_x^2 \{h_{\mathbf{k}} - (\xi_+ \xi_- - 2a_{3,+} a_{3,-} - 2a_{4,+} a_{4,-} - 2a_{5,+} a_{5,-}) f_{\mathbf{k}}\} - \frac{1}{N_\Lambda} \sum_{\mathbf{k}} s_x^2 \{h_{\mathbf{k}}^0 - \xi^2 f_{\mathbf{k}}^0\}, \quad (\text{A18})$$

$$\alpha'_4 = \frac{1}{N_\Lambda} \sum_{\mathbf{k}} c_y^2 \{h_{\mathbf{k}} - (\xi_+ \xi_- - 2a_{2,+} a_{2,-} - 2a_{4,+} a_{4,-}) f_{\mathbf{k}}\} - \frac{1}{N_\Lambda} \sum_{\mathbf{k}} s_y^2 \{h_{\mathbf{k}}^0 - \xi^2 f_{\mathbf{k}}^0\}, \quad (\text{A19})$$

$$\alpha''_1 = \frac{1}{N_\Lambda} \sum_{\mathbf{k}} s_x^2 \{h_{\mathbf{k}} - \xi_+ \xi_- f_{\mathbf{k}} - h_{\mathbf{k}}^0 + \xi^2 f_{\mathbf{k}}^0\}, \quad (\text{A20})$$

$$\alpha''_2 = \frac{1}{N_\Lambda} \sum_{\mathbf{k}} s_y^2 \{h_{\mathbf{k}} - (\xi_+ \xi_- - 2a_{2,+} a_{2,-} - 2a_{3,+} a_{3,-} - 2a_{5,+} a_{5,-}) f_{\mathbf{k}}\} - \frac{1}{N_\Lambda} \sum_{\mathbf{k}} s_y^2 \{h_{\mathbf{k}}^0 - \xi^2 f_{\mathbf{k}}^0\}, \quad (\text{A21})$$

$$\alpha''_3 = \frac{1}{N_\Lambda} \sum_{\mathbf{k}} s_y^2 \{h_{\mathbf{k}} - (\xi_+ \xi_- - 2a_{3,+} a_{3,-} - 2a_{4,+} a_{4,-} - 2a_{5,+} a_{5,-}) f_{\mathbf{k}}\} - \frac{1}{N_\Lambda} \sum_{\mathbf{k}} s_y^2 \{h_{\mathbf{k}}^0 - \xi^2 f_{\mathbf{k}}^0\}, \quad (\text{A22})$$

$$\alpha''_4 = \frac{1}{N_\Lambda} \sum_{\mathbf{k}} c_x^2 \{h_{\mathbf{k}} - (\xi_+ \xi_- - 2a_{2,+} a_{2,-} - 2a_{4,+} a_{4,-}) f_{\mathbf{k}}\} - \frac{1}{N_\Lambda} \sum_{\mathbf{k}} s_x^2 \{h_{\mathbf{k}}^0 - \xi^2 f_{\mathbf{k}}^0\}, \quad (\text{A23})$$

where $\frac{J_1^1}{4}$ were omitted from the overall factors in the right hand sides.

$$\beta_{1,2} = -\frac{1}{N_\Lambda} \sum_{\mathbf{k}} s_x s_y (a_{3,+} a_{5,-} + a_{5,+} a_{3,-}) f_{\mathbf{k}}, \quad (\text{A24})$$

$$\beta_{1,3} = -\frac{i}{N_\Lambda} \sum_{\mathbf{k}} s_x s_y (a_{4,-} g_{\mathbf{k}}^+ - a_{4,+} g_{\mathbf{k}}^-), \quad (\text{A25})$$

$$\beta_{1,5} = \frac{i}{N_\Lambda} \sum_{\mathbf{k}} s_x s_y (a_{2,-} g_{\mathbf{k}}^+ - a_{2,+} g_{\mathbf{k}}^-), \quad (\text{A26})$$

$$\beta_{1,7} = \frac{i}{N_\Lambda} \sum_{\mathbf{k}} s_x c_x (a_{2,+} a_{4,-} - a_{2,-} a_{4,+}) f_{\mathbf{k}}, \quad (\text{A27})$$

$$\beta_{2,4} = -\frac{i}{N_\Lambda} \sum_{\mathbf{k}} s_x s_y (a_{4,-} g_{\mathbf{k}}^+ - a_{4,+} g_{\mathbf{k}}^-), \quad (\text{A28})$$

$$\beta_{2,6} = \frac{i}{N_\Lambda} \sum_{\mathbf{k}} s_x s_y (a_{2,-} g_{\mathbf{k}}^+ - a_{2,+} g_{\mathbf{k}}^-), \quad (\text{A29})$$

$$\beta_{2,8} = \frac{i}{N_\Lambda} \sum_{\mathbf{k}} s_y c_y (a_{2,+} a_{4,-} - a_{2,-} a_{4,+}) f_{\mathbf{k}}, \quad (\text{A30})$$

$$\beta_{3,4} = \frac{1}{N_\Lambda} \sum_{\mathbf{k}} s_x s_y (a_{3,+} a_{5,-} + a_{3,-} a_{5,+}) f_{\mathbf{k}}, \quad (\text{A31})$$

$$\beta_{3,5} = \frac{1}{N_\Lambda} \sum_{\mathbf{k}} s_y^2 (a_{2,+} a_{4,-} + a_{2,-} a_{4,+}) f_{\mathbf{k}}, \quad (\text{A32})$$

$$\beta_{3,7} = -\frac{1}{N_\Lambda} \sum_{\mathbf{k}} c_x s_y (a_{2,+} g_{\mathbf{k}}^- + a_{2,-} g_{\mathbf{k}}^+), \quad (\text{A33})$$

$$\beta_{4,6} = \frac{1}{N_\Lambda} \sum_{\mathbf{k}} s_x^2 (a_{2,+} a_{4,-} + a_{2,-} a_{4,+}) f_{\mathbf{k}}, \quad (\text{A34})$$

$$\beta_{4,8} = -\frac{1}{N_\Lambda} \sum_{\mathbf{k}} s_x c_y (a_{2,+} g_{\mathbf{k}}^- + a_{2,-} g_{\mathbf{k}}^+), \quad (\text{A35})$$

$$\beta_{5,6} = \frac{1}{N_\Lambda} \sum_{\mathbf{k}} s_x s_y (a_{3,+} a_{5,-} + a_{3,-} a_{5,+}) f_{\mathbf{k}}, \quad (\text{A36})$$

$$\beta_{5,7} = -\frac{1}{N_\Lambda} \sum_{\mathbf{k}} c_x s_y (a_{4,+} g_{\mathbf{k}}^- + a_{4,-} g_{\mathbf{k}}^+), \quad (\text{A37})$$

$$\beta_{6,8} = -\frac{1}{N_\Lambda} \sum_{\mathbf{k}} s_x c_y (a_{4,+} g_{\mathbf{k}}^- + a_{4,-} g_{\mathbf{k}}^+), \quad (\text{A38})$$

$$\beta_{7,8} = -\frac{1}{N_\Lambda} \sum_{\mathbf{k}} c_x c_y (a_{3,+} a_{5,-} + a_{3,-} a_{5,+}) f_{\mathbf{k}}, \quad (\text{A39})$$

where $\frac{J_2^2}{4}$ were omitted from the overall factors in the right hand sides.

$$\beta_{1,9} = -\frac{\sqrt{2}}{N_\Lambda} \sum_{\mathbf{k}} s_x^2 c_y (a_{5,-} g_{\mathbf{k}}^+ + a_{5,+} g_{\mathbf{k}}^-), \quad (\text{A40})$$

$$\beta_{1,11} = -\frac{\sqrt{2}}{N_\Lambda} \sum_{\mathbf{k}} s_x s_y c_x (a_{5,-} g_{\mathbf{k}}^+ + a_{5,+} g_{\mathbf{k}}^-), \quad (\text{A41})$$

$$\beta_{2,9} = \frac{\sqrt{2}}{N_\Lambda} \sum_{\mathbf{k}} s_y s_x c_y (a_{3,-} g_{\mathbf{k}}^+ + a_{3,+} g_{\mathbf{k}}^-), \quad (\text{A42})$$

$$\beta_{2,11} = \frac{\sqrt{2}}{N_\Lambda} \sum_{\mathbf{k}} s_y s_y c_x (a_{3,-} g_{\mathbf{k}}^+ + a_{3,+} g_{\mathbf{k}}^-), \quad (\text{A43})$$

$$\beta_{3,9} = \frac{\sqrt{2}i}{N_\Lambda} \sum_{\mathbf{k}} s_y s_x c_y (a_{4,+} a_{5,-} - a_{5,+} a_{4,-}) f_{\mathbf{k}}, \quad (\text{A44})$$

$$\beta_{3,11} = \frac{\sqrt{2}i}{N_\Lambda} \sum_{\mathbf{k}} s_y s_y c_x (a_{4,+} a_{5,-} - a_{5,+} a_{4,-}) f_{\mathbf{k}}, \quad (\text{A45})$$

$$\beta_{3,10} = -\frac{\sqrt{2}}{N_\Lambda} \sum_{\mathbf{k}} s_y c_x c_y (a_{2,+} a_{5,-} + a_{5,+} a_{2,-}) f_{\mathbf{k}}, \quad (\text{A46})$$

$$\beta_{3,12} = \frac{\sqrt{2}}{N_\Lambda} \sum_{\mathbf{k}} s_y s_x s_y (a_{2,+} a_{5,-} + a_{5,+} a_{2,-}) f_{\mathbf{k}}, \quad (\text{A47})$$

$$\beta_{4,9} = \frac{\sqrt{2}i}{N_\Lambda} \sum_{\mathbf{k}} s_x s_x c_y (a_{3,+} a_{4,-} - a_{4,+} a_{3,-}) f_{\mathbf{k}}, \quad (\text{A48})$$

$$\beta_{4,11} = \frac{\sqrt{2}i}{N_\Lambda} \sum_{\mathbf{k}} s_x s_y c_x (a_{3,+} a_{4,-} - a_{4,+} a_{3,-}) f_{\mathbf{k}}, \quad (\text{A49})$$

$$\beta_{4,10} = \frac{\sqrt{2}}{N_\Lambda} \sum_{\mathbf{k}} s_x c_x c_y (a_{2,+} a_{3,-} + a_{3,+} a_{2,-}) f_{\mathbf{k}}, \quad (\text{A50})$$

$$\beta_{4,12} = -\frac{\sqrt{2}}{N_\Lambda} \sum_{\mathbf{k}} s_x s_x s_y (a_{2,+} a_{3,-} + a_{3,+} a_{2,-}) f_{\mathbf{k}}, \quad (\text{A51})$$

$$\beta_{5,9} = -\frac{\sqrt{2}i}{N_\Lambda} \sum_{\mathbf{k}} s_y s_x c_y (a_{2,+} a_{5,-} - a_{5,+} a_{2,-}) f_{\mathbf{k}}, \quad (\text{A52})$$

$$\beta_{5,11} = -\frac{\sqrt{2}i}{N_\Lambda} \sum_{\mathbf{k}} s_y c_x s_y (a_{2,+} a_{5,-} - a_{5,+} a_{2,-}) f_{\mathbf{k}}, \quad (\text{A53})$$

$$\beta_{5,10} = -\frac{\sqrt{2}}{N_\Lambda} \sum_{\mathbf{k}} s_y c_x c_y (a_{4,+} a_{5,-} + a_{5,+} a_{4,-}) f_{\mathbf{k}}, \quad (\text{A54})$$

$$\beta_{5,12} = \frac{\sqrt{2}}{N_\Lambda} \sum_{\mathbf{k}} s_y s_x s_y (a_{4,+} a_{5,-} + a_{5,+} a_{4,-}) f_{\mathbf{k}}, \quad (\text{A55})$$

$$\beta_{6,9} = \frac{\sqrt{2}i}{N_\Lambda} \sum_{\mathbf{k}} s_x s_x c_y (a_{2,+} a_{3,-} - a_{3,+} a_{2,-}) f_{\mathbf{k}}, \quad (\text{A56})$$

$$\beta_{6,11} = \frac{\sqrt{2}i}{N_\Lambda} \sum_{\mathbf{k}} s_x c_x s_y (a_{2,+} a_{3,-} - a_{3,+} a_{2,-}) f_{\mathbf{k}}, \quad (\text{A57})$$

$$\beta_{6,10} = \frac{\sqrt{2}}{N_\Lambda} \sum_{\mathbf{k}} s_x c_x c_y (a_{4,+} a_{3,-} + a_{3,+} a_{4,-}) f_{\mathbf{k}}, \quad (\text{A58})$$

$$\beta_{6,12} = -\frac{\sqrt{2}}{N_\Lambda} \sum_{\mathbf{k}} s_x s_x s_y (a_{4,+} a_{3,-} + a_{3,+} a_{4,-}) f_{\mathbf{k}}, \quad (\text{A59})$$

$$\beta_{7,10} = \frac{\sqrt{2}}{N_\Lambda} \sum_{\mathbf{k}} c_x c_x c_y (a_{5,-} g_{\mathbf{k}}^+ + a_{5,+} g_{\mathbf{k}}^-), \quad (\text{A60})$$

$$\beta_{7,12} = -\frac{\sqrt{2}}{N_\Lambda} \sum_{\mathbf{k}} c_x s_x s_y (a_{5,-} g_{\mathbf{k}}^+ + a_{5,+} g_{\mathbf{k}}^-), \quad (\text{A61})$$

$$\beta_{8,10} = -\frac{\sqrt{2}}{N_\Lambda} \sum_{\mathbf{k}} c_y c_x c_y (a_{3,-} g_{\mathbf{k}}^+ + a_{3,+} g_{\mathbf{k}}^-), \quad (\text{A62})$$

$$\beta_{8,12} = \frac{\sqrt{2}}{N_\Lambda} \sum_{\mathbf{k}} c_y s_x s_y (a_{3,-} g_{\mathbf{k}}^+ + a_{3,+} g_{\mathbf{k}}^-), \quad (\text{A63})$$

where $\frac{J_1 J_2}{4}$ were omitted from the overall factors in the right hand sides.

$$\beta_{9,11} = \frac{1}{N_\Lambda} \sum_{\mathbf{k}} 2s_x s_y c_x c_y \{ h_{\mathbf{k}} + \xi_+ \xi_- f_{\mathbf{k}} \}, \quad (\text{A64})$$

$$\beta_{10,12} = -\frac{1}{N_\Lambda} \sum_{\mathbf{k}} 2s_x s_y c_x c_y \{ h_{\mathbf{k}} - (\xi_+ \xi_- - 2a_{3,+} a_{3,-} - 2a_{5,+} a_{5,-}) f_{\mathbf{k}} \}, \quad (\text{A65})$$

$$\beta_{9,10} = \frac{2i}{N_\Lambda} \sum_{\mathbf{k}} s_x c_x c_y^2 (a_{2,+} a_{4,-} - a_{4,+} a_{2,-}) f_{\mathbf{k}}, \quad (\text{A66})$$

$$\beta_{9,12} = -\frac{2i}{N_\Lambda} \sum_{\mathbf{k}} s_x^2 s_y c_y (a_{2,+} a_{4,-} - a_{4,+} a_{2,-}) f_{\mathbf{k}}, \quad (\text{A67})$$

$$\beta_{10,11} = -\frac{2i}{N_\Lambda} \sum_{\mathbf{k}} c_x^2 s_y c_y (a_{2,+} a_{4,-} - a_{4,+} a_{2,-}) f_{\mathbf{k}}, \quad (\text{A68})$$

$$\beta_{11,12} = -\frac{2i}{N_\Lambda} \sum_{\mathbf{k}} s_x c_x s_y^2 (a_{2,+} a_{4,-} - a_{4,+} a_{2,-}) f_{\mathbf{k}}, \quad (\text{A69})$$

where $\frac{J_2^2}{4}$ were omitted from the overall factors in the right hand sides.

$$\beta'_{1,2} = -\frac{i}{N_\Lambda} \sum_{\mathbf{k}} s_x s_y (a_{4,-} g_{\mathbf{k}}^+ - a_{4,+} g_{\mathbf{k}}^-), \quad (\text{A70})$$

$$\beta'_{1,3} = \frac{i}{N_\Lambda} \sum_{\mathbf{k}} s_x s_y (a_{2,-} g_{\mathbf{k}}^+ - a_{2,+} g_{\mathbf{k}}^-), \quad (\text{A71})$$

$$\beta'_{1,4} = \frac{i}{N_\Lambda} \sum_{\mathbf{k}} s_y c_y (a_{2,+} a_{4,-} - a_{4,+} a_{2,-}) f_{\mathbf{k}}, \quad (\text{A72})$$

$$\beta'_{2,3} = \frac{1}{N_\Lambda} \sum_{\mathbf{k}} s_x^2 (a_{2,+} a_{4,-} + a_{4,+} a_{2,-}) f_{\mathbf{k}}, \quad (\text{A73})$$

$$\beta'_{2,4} = -\frac{1}{N_\Lambda} \sum_{\mathbf{k}} s_x c_y (a_{2,+} g_{\mathbf{k}}^- + a_{2,-} g_{\mathbf{k}}^+), \quad (\text{A74})$$

$$\beta'_{3,4} = -\frac{1}{N_\Lambda} \sum_{\mathbf{k}} s_x c_y (a_{4,+} g_{\mathbf{k}}^- + a_{4,-} g_{\mathbf{k}}^+), \quad (\text{A75})$$

$$\beta''_{1,2} = -\frac{i}{N_\Lambda} \sum_{\mathbf{k}} s_x s_y (a_{4,-} g_{\mathbf{k}}^+ - a_{4,+} g_{\mathbf{k}}^-), \quad (\text{A76})$$

$$\beta''_{1,3} = \frac{i}{N_\Lambda} \sum_{\mathbf{k}} s_x s_y (a_{2,-} g_{\mathbf{k}}^+ - a_{2,+} g_{\mathbf{k}}^-), \quad (\text{A77})$$

$$\beta''_{1,4} = \frac{i}{N_\Lambda} \sum_{\mathbf{k}} s_x c_x (a_{2,+} a_{4,-} - a_{4,+} a_{2,-}) f_{\mathbf{k}}, \quad (\text{A78})$$

$$\beta''_{2,3} = \frac{1}{N_\Lambda} \sum_{\mathbf{k}} s_y^2 (a_{2,+} a_{4,-} + a_{4,+} a_{2,-}) f_{\mathbf{k}}, \quad (\text{A79})$$

$$\beta''_{2,4} = -\frac{1}{N_\Lambda} \sum_{\mathbf{k}} s_y c_x (a_{2,+} g_{\mathbf{k}}^- + a_{2,-} g_{\mathbf{k}}^+), \quad (\text{A80})$$

$$\beta''_{3,4} = -\frac{1}{N_\Lambda} \sum_{\mathbf{k}} s_y c_x (a_{4,+} g_{\mathbf{k}}^- + a_{4,-} g_{\mathbf{k}}^+), \quad (\text{A81})$$

where $\frac{J_2^2}{4}$ were omitted from the overall factors in the right hand sides. In all of these equations, symbols are defined as $s_\mu \equiv \sin(k_\mu)$, $c_\mu \equiv \cos(k_\mu)$ with $\mu = x, y$, and

$$a_{2,\pm} \equiv J_2 \eta \sin\left(k_x \pm \frac{q_x}{2}\right) \sin\left(k_y \pm \frac{q_y}{2}\right), \quad (\text{A82})$$

$$a_{3,\pm} \equiv \frac{J_1 D}{2} \sin\left(k_x \pm \frac{q_x}{2}\right), \quad (\text{A83})$$

$$a_{4,\pm} \equiv J_2 \chi \cos\left(k_x \pm \frac{q_x}{2}\right) \cos\left(k_y \pm \frac{q_y}{2}\right), \quad (\text{A84})$$

$$a_{5,\pm} \equiv -\frac{J_1 D}{2} \sin\left(k_y \pm \frac{q_y}{2}\right), \quad (\text{A85})$$

$$a_2 \equiv J_2 \eta \sin k_x \sin k_y \quad a_3 \equiv \frac{J_1 D}{2} \sin k_x, \quad (\text{A86})$$

$$a_4 \equiv J_2 \chi \cos k_x \cos k_y, \quad a_5 \equiv -\frac{J_1 D}{2} \sin k_y, \quad (\text{A87})$$

$$f_{\mathbf{k}} \equiv \frac{1}{2} \frac{\xi_+ + \xi_-}{\xi_+ \xi_-} \frac{1}{\epsilon_n^2 + (\xi_+ + \xi_-)^2}, \quad (\text{A88})$$

$$g_{\mathbf{k}}^\pm \equiv \pm \frac{1}{2\xi_\mp} \frac{i\epsilon_n}{\epsilon_n^2 + (\xi_+ + \xi_-)^2}, \quad (\text{A89})$$

$$h_{\mathbf{k}} \equiv -\frac{1}{2} \frac{\xi_+ + \xi_-}{\epsilon_n^2 + (\xi_+ + \xi_-)^2}, \quad (\text{A90})$$

$$f_{\mathbf{k}}^0 \equiv \frac{1}{4\xi^3}, \quad h_{\mathbf{k}}^0 \equiv -\frac{1}{4\xi} \quad (\text{A91})$$

with

$$\xi_+ \xi_- \equiv \sum_{j=2}^5 a_{j,+} a_{j,-},$$

$$\xi_\pm \equiv \sqrt{\sum_{j=2}^5 a_{j,\pm}^2}, \quad \xi \equiv \sqrt{\sum_{j=2}^5 a_j^2}. \quad (\text{A92})$$

The vertex parts $\bar{\mathcal{S}}_{\mu;\mu}^{(1,1)}(\mathbf{q}, i\epsilon_n)$ ($\mu = 1, 2, 3$), defined in Eq. (66), are calculated as follows:

$$\bar{\mathcal{S}}_{3;3}^{(1,1)} \equiv \begin{pmatrix} \mathbf{e}_1^3 & \mathbf{e}_2^3 & \mathbf{e}_3^3 & \mathbf{e}_4^3 & \mathbf{e}_5^3 & \mathbf{e}_6^3 & \mathbf{e}_7^3 & \mathbf{e}_8^3 & \mathbf{e}_9^3 & \mathbf{e}_{10}^3 & \mathbf{e}_{11}^3 & \mathbf{e}_{12}^3 \\ \gamma_{3;1} & \gamma_{3;2} & \gamma_{3;3} & \gamma_{3;4} & \gamma_{3;5} & \gamma_{3;6} & 0 & 0 & \gamma_{3;9} & 0 & \gamma_{3;11} & 0 \end{pmatrix}, \quad (\text{A93})$$

$$\bar{\mathcal{S}}_{1;1}^{(1,1)} \equiv \begin{pmatrix} \mathbf{e}_1^1 & \mathbf{e}_2^1 & \mathbf{e}_3^1 & \mathbf{e}_4^1 \\ \gamma_{1;1} & \gamma_{1;2} & \gamma_{1;3} & 0 \end{pmatrix}, \quad (\text{A94})$$

$$\bar{\mathcal{S}}_{2;2}^{(1,1)} \equiv \begin{pmatrix} \mathbf{e}_1^2 & \mathbf{e}_2^2 & \mathbf{e}_3^2 & \mathbf{e}_4^2 \\ \gamma_{2;1} & \gamma_{2;2} & \gamma_{2;3} & 0 \end{pmatrix}, \quad (\text{A95})$$

where the coefficients take the forms

$$\gamma_{3;1} \equiv \frac{i}{N_\Lambda} \sum_{\mathbf{k}} s_x (a_{3,+} g_{\mathbf{k}}^- - a_{3,-} g_{\mathbf{k}}^+), \quad (\text{A96})$$

$$\gamma_{3;2} \equiv \frac{i}{N_\Lambda} \sum_{\mathbf{k}} s_y (a_{5,+} g_{\mathbf{k}}^- - a_{5,-} g_{\mathbf{k}}^+), \quad (\text{A97})$$

$$\gamma_{3;3} \equiv \frac{1}{N_\Lambda} \sum_{\mathbf{k}} s_y (a_{3,+} a_{4,-} + a_{3,-} a_{4,+}) f_{\mathbf{k}}, \quad (\text{A98})$$

$$\gamma_{3;4} \equiv \frac{1}{N_\Lambda} \sum_{\mathbf{k}} s_x (a_{5,+} a_{4,-} + a_{5,-} a_{4,+}) f_{\mathbf{k}}, \quad (\text{A99})$$

$$\gamma_{3;5} \equiv -\frac{1}{N_\Lambda} \sum_{\mathbf{k}} s_y (a_{2,+} a_{3,-} + a_{3,-} a_{2,+}) f_{\mathbf{k}}, \quad (\text{A100})$$

$$\gamma_{3;6} \equiv -\frac{1}{N_\Lambda} \sum_{\mathbf{k}} s_x (a_{2,+} a_{5,-} + a_{2,-} a_{5,+}) f_{\mathbf{k}}, \quad (\text{A101})$$

where $\frac{J_1}{4}$ were omitted from the overall factors in the right hand sides.

$$\gamma_{3;9} \equiv -\frac{\sqrt{2}i}{N_\Lambda} \sum_{\mathbf{k}} s_x c_y (a_{3,+} a_{5,-} - a_{3,-} a_{5,+}) f_{\mathbf{k}}, \quad (\text{A102})$$

$$\gamma_{3;11} \equiv -\frac{\sqrt{2}i}{N_\Lambda} \sum_{\mathbf{k}} c_x s_y (a_{3,+} a_{5,-} - a_{3,-} a_{5,+}) f_{\mathbf{k}}, \quad (\text{A103})$$

where $\frac{J_2}{4}$ were omitted from the overall factors in the right hand sides.

$$\gamma_{1;1} \equiv -\frac{i}{N_\Lambda} \sum_{\mathbf{k}} s_y (a_{5,+} g_{\mathbf{k}}^- - a_{5,-} g_{\mathbf{k}}^+), \quad (\text{A104})$$

$$\gamma_{1;2} \equiv -\frac{1}{N_\Lambda} \sum_{\mathbf{k}} s_x (a_{4,+} a_{5,-} + a_{4,-} a_{5,+}) f_{\mathbf{k}}, \quad (\text{A105})$$

$$\gamma_{1;3} \equiv \frac{1}{N_\Lambda} \sum_{\mathbf{k}} s_x (a_{2,+} a_{5,-} + a_{2,-} a_{5,+}) f_{\mathbf{k}}, \quad (\text{A106})$$

where $\frac{J_1}{4}$ were omitted from the overall factors in the right hand sides.

$$\gamma_{2;1} \equiv -\frac{i}{N_\Lambda} \sum_{\mathbf{k}} s_x (a_{3,+} g_{\mathbf{k}}^- - a_{3,-} g_{\mathbf{k}}^+), \quad (\text{A107})$$

$$\gamma_{2;2} \equiv -\frac{1}{N_\Lambda} \sum_{\mathbf{k}} s_y (a_{4,+} a_{3,-} + a_{4,-} a_{3,+}) f_{\mathbf{k}}, \quad (\text{A108})$$

$$\gamma_{2;3} \equiv \frac{1}{N_\Lambda} \sum_{\mathbf{k}} s_y (a_{2,+} a_{3,-} + a_{2,-} a_{3,+}) f_{\mathbf{k}}. \quad (\text{A109})$$

where $\frac{J_1}{4}$ were omitted from the overall factors in the right hand sides.

Appendix B: Mass of low-energy modes in $\text{Im}\chi_{zz}(\mathbf{q}, \epsilon)$ at $\mathbf{q} = (\pi, 0)$ and $(0, \pi)$

Low-energy excitations in the Z_2 planar phase consist of not only spin-wave (director-wave) modes at $\mathbf{q} = (0, 0)$ but also another gapless mode in $\text{Im}\chi_{zz}(\mathbf{q}, \epsilon)$ at $\mathbf{q} = (\pi, 0)$, i.e. \mathbf{e}_8^3 -mode. Inside the $U(1)$ planar phase, the mass of the latter mode becomes even negative, indicating an instability. A direct evaluation of the PRA propagator at $\mathbf{q} = (\pi, 0)$ and $i\epsilon_n = 0$ suggests that \mathbf{e}_8^3 -mode becomes decoupled from others and its mass is given by

α_8 ;

$$[\overline{\mathcal{S}}_{33}^{(0,2)}]_{\mathbf{q}=(\pi,0), \epsilon=0} \equiv \mathbf{e}_8^3 \begin{pmatrix} \cdots & \mathbf{e}_8^3 & \cdots \\ \vdots & \begin{pmatrix} \ddots & 0 & \ddots \\ 0 & \alpha_8 & 0 \\ \vdots & \ddots & 0 & \ddots \end{pmatrix} & \vdots \end{pmatrix} \quad (\text{B1})$$

at $\mathbf{q} = (\pi, 0)$ and $i\epsilon_n = 0$, where α_8 reads

$$\alpha_8 = -\frac{1}{N_\Lambda} \sum_{\mathbf{k}} \left(\frac{c_y^2}{\xi_+} - \frac{s_y^2}{\xi} \right) = -\frac{1}{N_\Lambda} \sum_{\mathbf{k}} \frac{c_y^2 - s_y^2}{\xi}, \quad (\text{B2})$$

$$\xi_+^2 = J_2^2 \eta^2 c_x^2 s_y^2 + J_2^2 \chi^2 s_x^2 c_y^2 + \frac{J_1^2 D^2}{4} (c_x^2 + s_y^2),$$

$$\xi^2 = J_2^2 \eta^2 x_x^2 s_y^2 + J_2^2 \chi^2 c_x^2 c_y^2 + \frac{J_1^2 D^2}{4} (s_x^2 + s_y^2).$$

One can see that α_8 given by Eq. (B2) is reduced to zero in the Z_2 planar phase, by noting that the mean-field gap equation for the pairing fields, D , χ and η , is given by the following coupled equations

$$J_1 D = \frac{1}{N_\Lambda} \sum_{\mathbf{k}} \frac{\partial \xi}{\partial D} \tanh\left(\frac{\beta \xi}{2}\right) = \frac{1}{N_\Lambda} \frac{J_1^2 D}{4} \sum_{\mathbf{k}} \frac{s_x^2 + s_y^2}{\xi},$$

$$J_2 \chi = \frac{1}{N_\Lambda} \sum_{\mathbf{k}} \frac{\partial \xi}{\partial \chi} \tanh\left(\frac{\beta \xi}{2}\right) = \frac{1}{N_\Lambda} J_2^2 \chi \sum_{\mathbf{k}} \frac{c_x^2 c_y^2}{\xi},$$

$$J_2 \eta = \frac{1}{N_\Lambda} \sum_{\mathbf{k}} \frac{\partial \xi}{\partial \eta} \tanh\left(\frac{\beta \xi}{2}\right) = \frac{1}{N_\Lambda} J_2^2 \eta \sum_{\mathbf{k}} \frac{s_x^2 s_y^2}{\xi}$$

at $\beta^{-1} = 0$. Namely, in the Z_2 phase ($\eta \neq 0$ and $\chi \neq 0$), this gap equation leads to

$$J_2^{-1} = \frac{1}{N_\Lambda} \sum_{\mathbf{k}} \frac{c_x^2 c_y^2}{\xi}, \quad J_2^{-1} = \frac{1}{N_\Lambda} \sum_{\mathbf{k}} \frac{s_x^2 s_y^2}{\xi}. \quad (\text{B3})$$

Or,

$$0 = \frac{1}{N_\Lambda} \sum_{\mathbf{k}} \frac{c_x^2 c_y^2 - s_x^2 s_y^2}{\xi} = \frac{1}{N_\Lambda} \sum_{\mathbf{k}} \frac{c_y^2 - s_y^2 - (s_x^2 c_y^2 - c_x^2 s_y^2)}{\xi}.$$

Since ξ is symmetric under the exchange between k_x and k_y , the right hand side leads to $\alpha_8 = 0$. In the $U(1)$ planar phase ($\eta = 0$ and $\chi \neq 0$), the gap equation leads to

$$J_2^{-1} = \frac{1}{N_\Lambda} \sum_{\mathbf{k}} \frac{c_x^2 c_y^2}{\xi}, \quad J_2^{-1} > \frac{1}{N_\Lambda} \sum_{\mathbf{k}} \frac{s_x^2 s_y^2}{\xi}. \quad (\text{B4})$$

instead of Eqs. (B3). This dictates that the mass of the \mathbf{e}_8^3 mode becomes negative, $\alpha_8 < 0$. Similarly, one can see from Eqs. (A15), (A17), and (A21) that the mass of \mathbf{e}_2^1 , \mathbf{e}_2^2 and \mathbf{e}_{12}^3 modes at $\mathbf{q} = (\pi, \pi)$ also become negative in the $U(1)$ planar phase.

- ¹ L. Balents, *Nature* **464**, 199 (2010); P. A. Lee, *Science* **321**, 1306 (2008).
- ² P. Fazekas and P. W. Anderson, *Philos. Mag.* **30**, 423 (1974); P. W. Anderson, *Science* **235**, 1196 (1987).
- ³ X. G. Wen, *Quantum Field Theory of Many-Body systems* (Oxford University Press, Cambridge 2003).
- ⁴ E. Fradkin, *Field Theories of Condensed Matter Systems*, (Addison-Wesley, 1991).
- ⁵ A. F. Andreev and A. Grishchuk, *Sov. Phys. LETP* **60**, 267 (1984).
- ⁶ A. V. Chubukov, *Phys. Rev. B* **44**, 4693 (1991).
- ⁷ T. Momoi and N. Shannon, *Prog. Theor. Phys. Suppl.* **159**, 72 (2005).
- ⁸ N. Shannon, T. Momoi, and P. Sindzingre, *Phys. Rev. Lett.* **96**, 027213 (2006).
- ⁹ R. Shindou and T. Momoi, *Phys. Rev. B* **80**, 064410 (2009).
- ¹⁰ T. Vekua, A. Honecker, H.-J. Mikeska, and F. Heidrich-Meisner, *Phys. Rev. B* **76**, 174420 (2007).
- ¹¹ T. Hikiyara, L. Kecke, T. Momoi, and A. Furusaki, *Phys. Rev. B* **78**, 144404 (2008).
- ¹² J. Sudan, A. Lüscher, and A.M. Läuchli, *Phys. Rev. B* **80**, 140402(R) (2009).
- ¹³ M. Sato, T. Momoi, and A. Furusaki, *Phys. Rev. B* **79**, 060406(R) (2009); M. Sato, T. Hikiyara, and T. Momoi, *Phys. Rev. B* **83**, 064405 (2011).
- ¹⁴ H. T. Ueda and K. Totsuka, *Phys. Rev. B* **80**, 014417 (2009).
- ¹⁵ M. E. Zhitomirsky and H. Tsunetsugu, *Europhys. Lett.* **91**, 37001 (2010).
- ¹⁶ T. Momoi, P. Sindzingre, and K. Kubo, *Phys. Rev. Lett.* **108**, 057206 (2012).
- ¹⁷ M. Sato, T. Hikiyara, and T. Momoi, *arxiv:1208.2235*.
- ¹⁸ A. V. Syromyatnikov, *Phys. Rev. B*, **86**, 014423 (2012).
- ¹⁹ H. T. Ueda and T. Momoi, *arxiv:arXiv:1111.3184*.
- ²⁰ L. E. Svistov, T. Fujita, H. Yamaguchi, S. Kimura, K. Omura, A. Prokofiev, A. I. Smirnov, Z. Honda, and M. Hagiwara, *J. Exp. Theo. Phys. Lett.* **93**, 24 (2011).
- ²¹ M. Mourigal, M. Enderle, B. Fak, R. K. Kremer, J. M. Law, A. Schneidewind, A. Hiess, and A. Prokofiev, *Phys. Rev. Lett.* **109**, 027203 (2012).
- ²² K. Nawa, K. Yoshimura, M. Yoshida, and M. Takigawa, private communication.
- ²³ For quantum spin nematic phases in (quasi)-one-dimensional spin systems, please refer to Ref. 13.
- ²⁴ This state was referred to as a two-dimensional analogue of the Balian-Werthamer state²⁵ in Ref. 9, but it is usually called the planar state in the context of superfluid ³He. We adopt the name “planar state” in this paper.
- ²⁵ R. Balian and N. R. Werthamer, *Phys. Rev.* **131**, 1553 (1963).
- ²⁶ R. Shindou, S. Yunoki, and T. Momoi, *Phys. Rev. B*, **84**, 134414 (2011).
- ²⁷ I. Affleck and J. B. Marston, *Phys. Rev. B* **37**, 3774 (1988); *Phys. Rev. B* **39**, 11538 (1989).
- ²⁸ J. Richter, R. Darradi, J. Schulenburg, D. J. J. Farnell, and H. Rosner, *Phys. Rev. B* **81**, 174429 (2010).
- ²⁹ A. Auerbach, *Interacting electrons and Quantum Magnetism* (Springer-Verlag, New York 1994).
- ³⁰ C. Herring, *Magnetism IV*, edited by G. T. Rado and H. Suhl, (Academic Press, 1966).
- ³¹ H. Tsunetsugu and M. Arikawa, *J. Phys. Soc. Jpn.* **75**, 083701 (2006); *Journal of Physics Condensed Matter*, **19**, 145248 (2007).
- ³² A. Läuchli, F. Mila, and K. Penc, *Phys. Rev. Lett.* **97**, 087205 (2006).
- ³³ X. G. Wen, *Phys. Rev. B* **44**, 2664 (1991); C. Mudry and E. Fradkin, *Phys. Rev. B* **49**, 5200 (1994).
- ³⁴ V. N. Popov, *Functional integrals and collective excitations* (Cambridge University Press, New York, 1999).
- ³⁵ D. Vollhardt and P. Wolfle, *The Superfluids Phases of Helium 3* (Taylor & Francis, 1990) and reference therein.
- ³⁶ W. P. Halperin and E. Varoquaux, *Helium Three* (Elsevier, Amsterdam 1990).
- ³⁷ A. M. Polyakov, *Nucl. Phys. B* **120**, 429 (1977).
- ³⁸ N. Read and S. Sachdev, *Phys. Rev. Lett.* **62**, 1694 (1989); *Phys. Rev. B* **42**, 4568 (1990).
- ³⁹ A ‘modulated’ spin liquid with the same antiferromagnetic ordering is recently discussed by; C. Pepin, M. Norman, S. Burdin, and A. Ferraz, *Phys. Rev. Lett.* **106**, 106601 (2011).
- ⁴⁰ A. Smerald and N. Shannon, unpublished.
- ⁴¹ T. Moriya, *Prog. Theor. Phys.* **16**, 23 (1956).
- ⁴² The energy-momentum dispersion for gapless spin-wave modes in a quasi-two-dimensional system generally has a weak dispersion in the third direction. The effective spatial dimension ‘*d*’ should be taken to be 2, when the temperature is sufficiently larger than a characteristic energy scale associated with this weak dispersion, whereas *d* should be 3, when the temperature is in the same order of this energy scale.
- ⁴³ A. Smerald and N. Shannon, *Phys. Rev. B* **84**, 184437 (2011).